JCI The Journal of Clinical Investigation

Pancreatic triglyceride lipase mediates lipotoxic systemic inflammation

Cristiane de Oliveira, … , Mark E. Lowe, Vijay P. Singh

J Clin Invest. 2020. https://doi.org/10.1172/JCI132767.

Research In-Press Preview Gastroenterology Inflammation

Graphical abstract

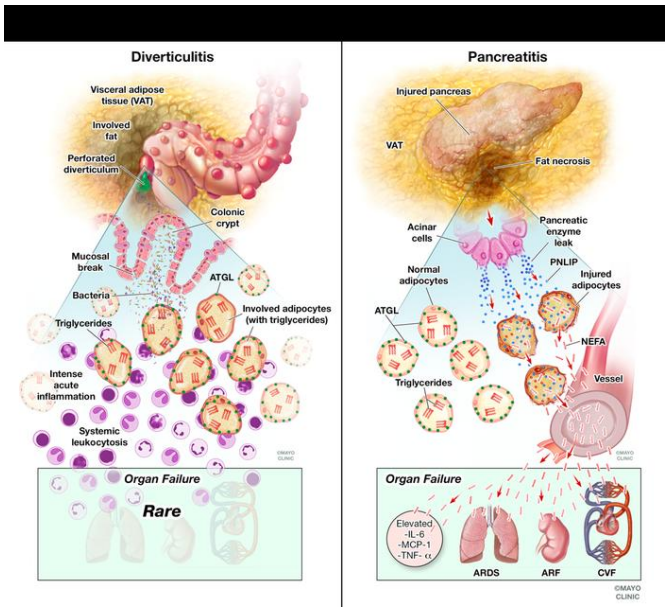

Find the latest version:

https://jci.me/132767/pdf

Pancreatic triglyceride lipase mediates lipotoxic systemic inflammation

Cristiane de Oliveira[1,7], Biswajit Khatua[1,7], Pawan Noel[1], Sergiy Kostenko[1], Arup Bag[1], Bijinu Balakrishnan[1], Krutika S. Patel[1], Andre A. Guerra[1], Melissa N. Martinez[1], Shubham Trivedi[1], Ann McCullough[2], Dora M. Lam-Himlin[2], Sarah Navina[3], Douglas O. Faigel[1], Norio Fukami[1], Rahul Pannala[1], Anna Evans Phillips[4], Georgios I. Papachristou[5], Erin E. Kershaw[4], Mark E. Lowe[6], Vijay P. Singh[1,*]

[1]Department of Medicine, Mayo Clinic, Scottsdale, Arizona, USA

[2]Department of Laboratory Medicine and Pathology, Mayo Clinic, Rochester, Minnesota, USA

[3]Department of Pathology, University of Pittsburgh School of Medicine, Pittsburgh, Pennsylvania, USA

[4]Department of Medicine, University of Pittsburgh School of Medicine, Pittsburgh, Pennsylvania, USA

[5]Department of Medicine, Ohio State University College of Medicine, Columbus, Ohio, USA

[6]Department of Pediatrics, Washington University Saint Louis, St. Louis, Missouri, USA

[7]Share the first-author position

Conflicts of Interest and Sources of Funding: The authors have declared that no conflicts of interest exist.

***Corresponding Author:**

Vijay P. Singh, MD

Division of Gastroenterology and Hepatology

Mayo Clinic

13400 East Shea Blvd.

Scottsdale, AZ 85259

Phone: 480-301-4286, Fax: 480-301-7017

Email: singh.vijay@mayo.edu

Abstract: Visceral adipose tissue plays a critical role in numerous diseases. While imaging studies often show adipose involvement in abdominal diseases, their outcomes may vary from being a mild self limited illness to one with systemic inflammation and organ failure. We therefore compared the pattern of visceral adipose injury during acute pancreatitis and acute diverticulitis to determine its role in organ failure. Acute pancreatitis-associated adipose tissue had ongoing lipolysis in the absence of adipocyte triglyceride lipase (ATGL). Pancreatic lipase injection into mouse visceral adipose tissue hydrolyzed adipose triglyceride and generated excess non-esterified fatty acids (NEFA), which caused organ failure in the absence of acute pancreatitis. Pancreatic triglyceride lipase (PNLIP) increased in adipose tissue during pancreatitis and entered adipocytes by multiple mechanisms, hydrolyzing adipose triglyceride and generating excessive NEFA. During pancreatitis, obese *PNLIP* knockout mice, unlike obese adipocyte-specific *ATGL* knockouts, had lower visceral adipose tissue lipolysis, milder inflammation, lesser organ failure, and improved survival. *PNLIP* knockout mice, unlike *ATGL* knockouts, were protected from adipocyte-induced pancreatic acinar injury without affecting NEFA signaling or acute pancreatitis induction. Therefore during pancreatitis, unlike diverticulitis, PNLIP leaked into visceral adipose tissue can cause excessive visceral adipose tissue lipolysis independent of adipocyte-autonomous ATGL, and thereby worsen organ failure.

Introduction:

In humans, visceral adipose tissue is commonly involved in acute diseases like acute diverticulitis (1, 2), appendicitis (3, 4), and acute pancreatitis (5-7), but the extent of visceral adipose involvement only parallels acute pancreatitis severity (1-7). This involvement is commonly imaged as “stranding” around the inflamed organs. While both acute diverticulitis and acute pancreatitis have a sudden onset, involve visceral fat, and occur in a similar demographic, diverticulitis is often treated in the outpatient setting and rarely causes organ failure (8), whereas

acute pancreatitis requires hospitalization and has a higher risk of progression to organ failure (9). The mechanisms underlying these differences are unknown.

Visceral fat necrosis worsens acute pancreatitis outcomes (10-14) in obesity. However, models mimicking acute diverticulitis (e.g., cecal ligation, puncture) have variable outcomes in obese mice (15, 16), with some reporting that visceral adipose tissue plays a protective role (17). A clue to this discrepancy may lay in acute non-esterified fatty acids (NEFA) elevations in acute pancreatitis (18, 19). High NEFAs can inhibit mitochondrial complexes I and V, cause necrosis of the pancreas, renal tubular injury, acute respiratory distress syndrome (ARDS), and result in multi-system organ failure (MSOF) (13, 14, 20). NEFA infusion can induce renal injury (21, 22) and acute respiratory distress syndrome (23, 24). The lipase mediating this rapid and excessive NEFA generation is therefore of interest.

Lipolysis within adipocytes is normally a highly regulated process involving adipocyte triglyceride lipase (ATGL) and hormone-sensitive lipase (25). The pancreas itself has 3 lipases: pancreatic triglyceride lipase (*PNLIP*); the major contributor to the pancreas' lipolytic activity (26, 27), pancreatic lipase-related protein-2 (PNLIPRP2), and carboxyl ester lipase (CEL) (28). These normally digest dietary fat in the intestine. While pharmacologic lipase inhibition improves pancreatitis outcomes (13, 14), whether adipocyte or pancreatic lipases mediate this NEFA generation is unknown. ATGL is normally the initiating and rate-limiting lipolytic enzyme in adipocytes (29). Its adipocyte-specific deletion decreased adipocyte lipolysis and serum lipids (30) in mice. More recently, pharmacologic inhibition of ATGL has been shown to slow progression of heart failure in mice (31). Since cardiovascular failure, shock (32, 33), and lipotoxicity from NEFAs (14, 34) can contribute to severe acute pancreatitis, we therefore also considered whether ATGL can mediate severe acute pancreatitis.

We therefore started by comparing the pathophysiology of NEFA generation in human acute diverticulitis to acute pancreatitis, and roles of pancreatic lipases vs. ATGL in the progression to organ failure. For this we used *in vitro* and *in vivo* models of acute pancreatitis, and tested the

efficacy of the specific ATGL inhibitor Atglistatin(35), an adipocyte-specific *ATGL* deletion (36), or genetic deletion of *PNLIP* (37) in preventing the cascade of lipolysis resulting in organ failure. Since carboxyl ester lipase cannot hydrolyze long chain triglycerides, such as those present in visceral fat (38-40), it was not studied.

Genetically obese mice, homozygous for mutant leptin (B6.Cg-*Lep*^{ob}/J; *ob/ob*), have increased visceral fat (41) and unlike lean mice develop pancreatitis associated multi-system organ failure similar to human severe acute pancreatitis (10, 13, 42). Therefore we mated *ATGL* or *PNLIP* knock outs with the leptin mutants to generate dual "*ATGL* floxed Cre positive (*ATGL* KO) ob/ob mice" or "*PNLIP* knockout (*PNLIP* KO) ob/ob" mice. These KO ob/ob mice matched the control ob/ob littermates in physical parameters and body composition. This allowed us to study the lipase(s) causing acute lipolysis of visceral adipose tissue and consequent local and systemic lipotoxic injury during acute pancreatitis. Interestingly, we note that acute visceral adipose tissue lipolysis changes pancreatitis outcomes without affecting its initiation independent of the mechanisms regulating lipolysis within adipocytes.

Results:

During human acute pancreatitis unlike diverticulitis, PNLIP accumulates in visceral adipose tissue and may hydrolyze it

Since both acute pancreatitis and acute diverticulitis have a sudden onset, involve visceral fat, and occur in a similar demographic but have very different outcomes, we first aimed to understand why visceral adipose tissue involvement during acute pancreatitis can worsen it, unlike diverticulitis. For this we compared the fat necrosis of acute pancreatitis to that of diverticulitis. An example of CT appearance of visceral adipose tissue involvement at the time of diagnosing acute diverticulitis or acute pancreatitis is shown in Figure 1 A-D. The day from disease onset is mentioned below the images. While both diseases had visceral adipose tissue involvement around the colon (C) and pancreas (P) respectively (yellow outline Fig. 1 A-D), this

increased in size over time during acute pancreatitis (Fig. 1 B-D). Patients with acute pancreatitis had a higher prevalence of organ failure than those with acute diverticulitis (5/8 vs. 0/8, p=0.03) despite being younger (Table in Fig. S1). The interval from the onset of disease to the time of surgery averaged 2 months in both cases (Fig. S1). We then analyzed the visceral fat samples removed at the time of surgery for these diseases. Uninvolved fat was not tested.

Histologically, acute diverticulitis showed intense adipose tissue acute inflammation with myeloperoxidase positive infiltrate (Fig. 1E). However, the adipocytes appeared normal (Fig. 1F) and stained negative for calcium (no black staining in von-Kossa; Fig. 1 G) and PNLIP (Fig. 1H). On a 0-3 scale, a blinded pathologist scored these 0 and 0-1 respectively in diverticulitis (Table in Fig. 1I). Fat necrosis during acute pancreatitis bordered pancreatic necrosis and, appeared chalky pink on H&E staining as shown previously (Fig. 1J) (14, 43). The necrosed adipocytes, unlike normal ones (green outline), stained positive for calcium (black stain, black arrows in Fig. 1K, scored as 3/3), consistent with saponified NEFA in the fat necrosis (14, 43). Serial sections scored 3/3 for PNLIP (brown arrows in brown areas, (Fig. 1L), in von-Kossa positive areas, unlike the fat in diverticulitis. Thus there was a histologic evidence of PNLIP leakage from the pancreatitis into fat necrosis (Fig. 1L) unlike during diverticulitis (Fig. 1F-H). This has been noted previously in human (44-46) and experimental pancreatitis (47-49).

On thin layer chromatography, the involved fat in acute diverticulitis remained predominantly triglyceride (Fig. 1M), but was hydrolyzed to NEFA in acute pancreatitis, with NEFA concentrations of 3.5±2.9mM. Similar to previous reports (14), oleic acid (C18:1) was the principal NEFA, comprising 38±10%. The fat in acute pancreatitis contained higher activity of pancreatic lipase, amylase, and trypsin compared diverticulitis (Fig. 1N-P). Interestingly, on western blotting, there was no detectable ATGL or perilipin-1 protein in the fat necrosis, while these proteins were present in diverticulitis (Fig. 1Q). Adiponectin was used as a marker for adipocytes and was present in both pancreatitis and diverticulitis. This result suggested that acute pancreatitis caused leakage of pancreatic hydrolases into the visceral adipose tissue,

which degraded proteins and triglycerides normally present in visceral adipose tissue. Such leakage has previously been shown in human pancreatitis (44-46) and experimental pancreatitis (47-49). Overall, these findings supported the need to verify that visceral adipose tissue could undergo lipolysis independent of ATGL, and to understand the mechanisms underlying this lipolysis which results in organ failure.

Pancreatic lipase hydrolyzes visceral adipose tissue causing fat necrosis, organ failure, and worsening inflammation

We went on to investigate whether a non-adipocyte lipase can cause visceral adipose tissue necrosis and organ failure. For this we first injected pancreatic lipase extracted from pigs (50) into the fat pads of ob/ob mice alone or along with the lipase inhibitor orlistat. Lipase injection dramatically reduced survival over 24 hours (Fig. 2A). Grossly, there was fat necrosis seen as round white deposits all over the visceral fat of the lipase treated mice, which was prevented by orlistat (Fig. 2B). The lipase injection also increased fat pad pancreatic lipase activity (Fig. 2C), and hydrolyzed adipocyte triglyceride into to NEFA (Fig. 2D). This lipolysis resulted in a 66±44-fold increase in various long chain NEFAs in visceral fat, with oleic acid (C18:1) being the main one (84±44 fold, Fig. 2E). All these changes were prevented by orlistat. This lipolysis also resulted in a large increase in serum cytokines IL6, MCP-1 and TNF-α (# Fig. 2F-H) and blood urea nitrogen elevation signifying renal injury (Fig. 2I), which were measured at the time of euthanasia. These increases were prevented or reduced by orlistat (* Fig. 2F-I). Additionally, lipolysis caused a large drop in rectal temperature and carotid pulse distension implying hypothermia and shock (Fig. 2J, K), which are a part of the severe systemic inflammatory response syndrome. These parameters, which were measured 12-16 hours after injection and before euthanasia was initiated, were also normalized by lipase inhibition.

Since NEFA generation immediately follows lipolysis, we went on to test whether NEFA alone could result in an inflammatory response and organ failure. Noting oleic acid (OA; C18:1)

to comprise a high proportion of NEFA in both human pancreatic necrosis collections and fat necrosis in mice, we studied the effect of administering OA to lean (CD-1) mice. OA (0.3% body weight), when given intraperitoneally to simulate visceral fat necrosis, increased serum OA concentrations (311±103μM vs. 132±53μM in controls $p<0.003$, Fig. 3A). OA-treated mice became progressively less active, requiring euthanasia at 48±13 hours. At this time there was a large increase noted in serum cytokines IL-6, MCP-1 and TNF-α (shown as * in Fig. 3B-D) and BUN (Fig. 3E) in the OA-treated group versus controls. Prior to euthanasia the OA-treated mice were in shock and hypothermic (Fig. 3F, G).OA treatment increased TUNEL positive cells in the lung from 0.2±0.1% to 2.7±1.4%, $p<0.001$ (Fig. 3H) similar to acute respiratory distress syndrome in rodents (24) and humans (51).

To test the clinical relevance of our findings with OA in a blinded fashion, OA concentrations were measured in a separate cohort of patients at the University of Pittsburgh detailed in table 1. Some of these had severe acute pancreatitis, which is characterized by the presence of organ failure for more than 48 hours (52). OA levels in severe acute pancreatitis patients (n=15) were significantly higher versus normal controls (n=15) who were demographically similar (Fig. 3I). OA levels in patients were similar to the levels noted in OA treated and control CD-1 mice (Fig. 3A).

Cumulatively these showed that during acute pancreatitis, unlike diverticulitis, pancreatic lipase can hydrolyze visceral adipose tissue, generate NEFA, which cause multi-system organ failure independent of intra-pancreatic phenomena. We further validated these findings using the standard caerulein acute pancreatitis model in lean and obese (ob/ob) mice. In ob/ob mice, fat necrosis was first noted at 12 hours near the pancreas (Fig. S2A, red rectangles). This increased in amount and distance from the pancreas over time and appeared similar to what was noted after lipase injection (Fig. 2B). Increased PNLIP and PNLIPRP2 were noted in the fat by 6h (Fig. S2B), and reduced amount of ATGL, perilipin-1 (Fig. S2K) were noted after 12h,

which correlated with an increase in pancreatic enzymes like trypsin and amylase in the fat necrosis (Figure S2L). Trypsin has been previously shown to hydrolyze ATGL (53). Circulating amylase and lipase activity, which are markers of ongoing acute pancreatitis, were similarly elevated during acute pancreatitis (Fig. S2C, D) in ob/ob and lean C57BL/6J mice (in pink). However, unlike lean mice (body fat 2.8±0.2 gm vs. 17.1±1.8gm) who developed little or no fat necrosis and organ failure (Fig. S3), serum NEFAs increased in ob/ob mice (Fig. S2E) in parallel with serum IL-6, MCP-1, TNFα, blood urea nitrogen, and reduced survival (Fig. S2F-J).

To understand how pancreatic lipases enter adipocytes, we exposed 3T3-LI cells to PNLIP-mcherry in the presence of phospholipase A2, several isoforms of which are involved in acute pancreatitis (54-56). This allowed the entry of PNLIP into the adipocytes (Fig. S4A). Similarly, PNLIPRP2, which has a phospholipase like activity (27), allowed the entry of a live/dead marker into these cells (Fig. S4B). The injurious role of PNLIPRP2 (unlike its inactive S148G mutant or PNLIP) was supported by its expression in HEK293 cells causing a significant increase in LDH leakage vs. PNLIP(Fig. S4C). Lastly, exposure of 3T3-L1 adipocytes to linoleic acid previously shown to be present at ≈2 mM in acute pancreatitis collections also injured adipocytes leading to entry of PNLIP into the cells (Fig. S4D). Thus, pancreatic enzymes including lipases which may leak from a disrupted duct(57, 58), or basolaterally during human (44-46) and experimental pancreatitis (47-49) can enter the surrounding visceral adipocytes in multiple ways and cause organ failure. We, therefore, went on to identify the relative contribution of pancreatic lipases versus ATGL to acute pancreatitis-associated fat necrosis, and consequent pancreatic acinar necrosis, the source of pancreatic lipase leak.

Pharmacological inhibition or genetic deletion of *ATGL* is not sufficient to prevent adipocyte-induced lipotoxic acinar injury

As previously shown, NEFA injure pancreatic acini (14, 59) and other cell types such as the kidney cell line HEK293 (40). To initially identify the lipase(s) mediating the cell injury resulting

from fat necrosis, we used a previously described method (14, 43). Using this method, we co-cultured wild type adipocytes and pancreatic acini alone or in the presence of Atglistatin (50μM); the ATGL-specific inhibitor (35) which does not inhibit pancreatic lipases or the generic lipase inhibitor orlistat (50μM; Fig. 4A-D). As previously shown (14, 43) during co-culture, these were separated by a 3μM pore size mesh (Fig. 4A). This system therefore allows the macromolecules released from one cell type to interact with the other cell type, thus simulating the leak of pancreatic lipases into adipose tissue noted previously during human (44-46) and mouse acute pancreatitis (14, 43). This model is relevant to the current study (Figs. 1, 2, S2-S4) since it allows the leaked pancreatic enzymes access to adipocytes and their triglyceride in the lower chamber (Fig. 4A), and conversely allows glycerol and NEFAs from adipocytes access to acini in the upper chamber, where these molecules can be measured. Injury to acini (or its prevention thereby) can thus be measured by staining the acini in the upper chamber with a live/dead marker such as trypan blue or propidium iodide, as shown previously (14, 43).

We initially noted the generic lipase inhibitor orlistat inhibited pancreatic lipase activity, reduced the lipolytic generation of glycerol and consequent lipotoxic necrosis of acini (14), as measured by their uptake of propidium iodide and trypan blue (Fig. 4B-E). Atglistatin however did not inhibit these phenomena despite potent inhibition of isoproterenol induced lipolysis (Fig. S5). In contrast, the medium in which *PNLIP* KO acini were suspended had reduced pancreatic lipase compared to medium from wild type acini, whereas amylase activity in the two media was similar (Fig. 4F). Co-culture of *PNLIP* KO acini with wild type adipocytes reduced glycerol generation, propidium iodide uptake, and trypan blue staining (Fig. 4G-I). While adipocytes from *ATGL* KO acini did have reduced lipolytic response to isoproterenol as previously shown (Fig. S5) (30), co-culture of adipocytes from *ATGL* KO mice with wild type acini caused no reduction in pancreatic lipase activity, glycerol generation, or protection from acinar necrosis (Fig. 4J-M). These data suggest that PNLIP, rather than ATGL, mediates the unregulated lipolysis of

adipocyte triglyceride, its subsequent NEFA release, and lipotoxic cell injury (14, 43). These findings along with 1) *in vivo* evidence that visceral fat necrosis is mediated by pancreatic lipases (Fig. 2), and contains PNLIP, PNLIPRP2 but less ATGL (Fig. 1 J-K, O, Q; Fig. S2B); 2) visceral fat necrosis generates NEFA (Fig. 1M; Fig. 2D, E); 3) NEFA cause organ failure (Fig. 3A-H); and 4) NEFA are increased in the sera (Fig. 3I) and pancreatic collections of patients with severe acute pancreatitis (14, 20, 60), but not diverticulitis (Fig. 1M) in whom organ failure is rare led us to compare the role of pancreatic lipases and ATGL in mediating the organ failure of severe acute pancreatitis *in vivo*.

PNLIP (but not PNLIPRP2) mediates lipotoxic NEFA generation without affecting lipotoxic NEFA signaling

We first chose to identify the pancreatic lipase to be targeted. Pancreatic necrosis collections are enriched in NEFA with 16 or more carbons (14, 34, 60) such as OA and linoleic acid. Triglycerides esterified to these long-chain fatty acids serve as poor substrates for the bile salt-dependent carboxyl ester lipase (CEL) (38-40). Thus we focused our attention on PNLIP (black/white/grey) and PNLIPRP2 (burgundy/ dirty yellow) by comparing their relative contributions in lipolytic release of lipotoxic mediators relevant to acute pancreatitis (Fig. 5). At equimolar amounts, both enzymes from mice, similar to the human forms (40), were effective in hydrolyzing the triglyceride of linoleic acids (LA), i.e., glyceryl trilinoleate (GTL; Fig. 5A, B). The lipase activity in pancreatic homogenates of *PNLIP* KO mice however was only 10% of the wild type mice (Fig. 5C), in contrast to the activity in homogenates of *PNLIPRP2* WT and KO mice, which were similar. Consistent with this finding, *PNLIPRP2* WT and KO acini had similar glycerol generation and injury (LDH leakage) after 2h of incubation with 300 μM GTL (Fig. 5D, E). *PNLIP* KO acini, however, generted less glycerol and cause less injury than wild type acini (Fig. 5F, G) despite being equally susceptible to the direct lipotoxic effect of LA (600 μM). Real

time analysis of mitochondrial depolarization and cytosolic calcium increase (Fig. 5H, I) revealed *PNLIP* KO acini to have a blunted response to GTL, while responding similarly to LA. These protective effects were not due to a generic decrease in exocrine enzyme release by the cells since only the lipase activity, but not amylase activity, was reduced in the medium of the *PNLIP* KO acini resulting in a reduced NEFA generation (Fig. 5J-L). Thus, the protection in *PNLIP* KO acini is by reducing triglyceride lipolysis and not by interference with the lipotoxic mechanisms of NEFA. We next sought to compare the role of PNLIP versus ATGL in severe acute pancreatitis-associated fat necrosis using obese *ATGL* KO or obese *PNLIP* KO mice.

Deficiency of *PNLIP*, but not *ATGL*, prevents visceral adipose tissue lipolysis during severe acute pancreatitis and improves outcomes

To confirm homogeneity between different animal groups, we first compared the body weight, adipose weights, and fatty acid composition of the gonadal fat pads (that get necrosed) of ob/ob *ATGL* KO and ob/ob *PNLIP* KO mice and their ob/ob littermates (Fig. 6A, B). These parameters were similar in all three groups. Similarly, the increase in pancreatic edema (measured as % water weight/tissue wet weight) and circulating amylase 24h after induction of pancreatitis were similar in all three groups (Fig. 6C, D). These results indicate that all groups had a similar susceptibility to acute pancreatitis. The *PNLIP* KO group, however, had lower circulating pancreatic lipase levels at baseline and throughout the course of acute pancreatitis (Fig. 6E). During acute pancreatitis, ob/ob mice and ob/ob *ATGL* KO mice developed comparable fat necrosis involving about 1/3rd of the fat in and around the pancreas (Fig. 6F, G; Figs. S6, S7). The pancreas adjacent to the fat necrosis was also similarly necrosed (referred to as perifat acinar necrosis, PFAN; yellow rectangles Fig. 6F); contributing to half the acinar necrosis. These findings are morphologically similar to human acute pancreatitis (Fig. 1 J-L) and supported by previous studies in humans (14, 43). Obese *PNLIP* KO mice however had dramatically reduced fat necrosis, PFAN, and total necrosis (Fig. 6F, G; Figs. S6, S7). These

results are supported by findings of the triglyceride in fat pads of the *PNLIP* KO mice being unhydrolyzed (Fig. S8A). Instead, by the 5th day of pancreatitis, when these mice were electively sacrificed, they had developed acinar-ductal metaplasia (ADM) involving about half the pancreas and extensive fibrosis (Figs. S8B, S9), consistent with sustained caerulein pancreatitis, which can progress to chronic pancreatitis (61, 62). These findings suggested that genetic deletion of *PNLIP* does not affect the induction of acute pancreatitis by caerulein but rather influences the progression via protection from fat necrosis.

In contrast to *PNLIP*, the lack of ATGL's role in lipolytic fat necrosis during acute pancreatitis was further supported by the ob/ob *ATGL* KO mice having grossly visible visceral fat necrosis similar to the ob/ob mice (Fig. 7A) with pancreatitis. *ATGL* KO mice had a similar increase in pancreatic lipase activity (Fig. 7B) and PNLIP (Fig. 7C) in the visceral fat by western blotting, along with an increase in serum C18:1 levels (Fig. 7D), unlike ob/ob *PNLIP* KO mice with acute pancreatitis. Interestingly, the serum C18:1 (i.e., oleic acid) levels in ob/ob mice with pancreatitis (276±60μM) and *ATGL* KO mice with pancreatitis (296±92μM) were similar to those noted in humans with severe AP (Fig. 3I) and CD-1 mice administered oleic acid (Fig. 3A). *ATGL* KO mice pancreatitis also had a similar pattern of proinflammatory cytokine mRNA in visceral adipose tissue and serum to the ob/ob mice with pancreatitis (Fig. 7E-H). Similarly, systemic injury reflected by elevated BUN, kidney and lung TUNEL positivity, shock (noted as a drop in carotid artery pulse distension), and/or hypothermia were equally severe in the ob/ob and ob/ob *ATGL* KO mice with acute pancreatitis (Figs. 7I-L, S10). This was unlike in the ob/ob *PNLIP* KO mice, whose parameters for organ failure, even at the end of the study, were no different from control mice without acute pancreatitis and which had a 100% survival (Fig. 7M).

We went on to test whether the role of PNLIP was relevant to a mechanistically different acute pancreatitis model using IL12, 18 (Fig. S11), which are cytokines increased in human severe acute pancreatitis (63, 64). All ob/ob mice with acute pancreatitis were moribund by day 4 post-induction (Fig. S11A), as shown previously. Ob/Ob *PNLIP* KO mice, however, were fully

protected over the 5-day course of the study and had near normal circulating amylase and lipase (Fig. S11B, C) at the time of elective euthanasia. On necropsy, these mice had grossly reduced visceral fat necrosis and no increase in measureable lipase activity in the fat pads (Fig. 11D, G). This was verified microscopically and was associated with reduced pancreatic necrosis (Fig. S11E, F), even though acinar-ductal metaplasia (ADM) was increased. The severe visceral adipose tissue necrosis was associated with a large increase in circulating NEFAs, including C18:1, and a severe inflammatory response, both of which were reduced in the *PNLIP* KO mice (Fig. S11H-K). Additioanally, ob/ob *PNLIP* KO mice with IL12, 18 induced acute pancreatitis were protected from renal failure, shock, and hypothermia (Fig. S11L-N), all of which occurred in the ob/ob mice prior to them becoming moribund. Therefore, PNLIP lipolytically worsens fat necrosis and acute pancreatitis outcomes in two mechanistically distinct acute pancreatitis models.

Deficiency of PNLIP activity does not affect the signaling that leads to the initiation of acute pancreatitis

Since acute pancreatitis is initiated in pancreatic acinar cells (65), we went on to check whether *PNLIP* affected the induction of acute pancreatitis by comparing the signaling induced by caerulein in the acini of WT and *PNLIP* KO mice (grey, Fig 8A-C). Caerulein acts via the cholecystokinin receptor and at high doses (>10^{-9} M) relevant to acute pancreatitis, it causes a sustained increase in cytosolic calcium (66, 67). The two types of acini showed no difference in the caerulein induced increase in cytosolic calcium, pattern of exocrine enzyme amylase secretion, or the generation on trypsin (Fig. 8A-C). Thus the protection seen in the ob/ob *PNLIP* KO mice during caerulein acute pancreatitis is not due to interference with the caerulein signaling leading to acute pancreatitis or the function of cells in which acute pancreatitis is initiated. We further went on to study the validity of this *in vivo* by comparing lean wild type and lean *PNLIP* KO mice during a short 10-hour course of caerulein acute pancreatitis. Here, the

PNLIP KO mice were not protected from the increase in circulating amylase (Fig. 8D), pancreatic edema (measured as % water weight/wet weight; Fig. 8E), and acinar necrosis (arrows showing diffuse pink cytoplasm and loss of cell outlines Fig. 8F), despite preventing the increase in circulating lipase compared to wild type mice (Fig. 8G). Consistent with the short course of acute pancreatitis and relative paucity of visceral adipose tissue in lean mice, neither strain had an increase in serum NEFA, blood urea nitrogen, or loss of thermoregulation with acute pancreatitis (Fig. S12A-C). Similarly, during IL12, 18 pancreatitis, *PNLIP* KO mice had a similar increase in serum amylase at 24 hours and pancreatic edema versus the wild type mice (Fig. 8H, I). However, the increase in circulating lipase was completely prevented in the *PNLIP* KO mice (Fig. 8J). Again, serum BUN and rectal temperature were similar (Fig. S12D, E) between WT and *PNLIP* KO mice. Based on these findings, we can conclude that the protection noted in the *PNLIP* KO mice is not due to interference with the initiation of acute pancreatitis. Rather these mice are protected from the lipotoxicity that ensues from excessive visceral adipose tissue lipolysis mediated by the leakage of PNLIP into the visceral adipose tissue (Fig. 9), which causes systemic inflammation and organ failure.

Discussion:

In this study we note that acute, excessive visceral adipose tissue lipolysis by pancreatic lipase can cause systemic injury, and then identify PNLIP as the principal lipase mediating this during acute pancreatitis. This explains the higher prevalence of organ failure in acute pancreatitis compared to diverticulitis, despite both diseases being acute, occurring in a similar demographic, and having visceral fat involvement. Diverticulitis however does not have ongoing visceral fat lipolysis despite the radiographically apparent visceral fat involvement and intense inflammation seen histologically. As summarized in Figure 9, these studies show that during acute pancreatitis, PNLIP leaks from the injured pancreas into the surrounding adipocytes with its entry facilitated by multiple mechanisms (Fig. S4). PNLIP mediated lipolysis results in the

release of large quantities of NEFA like oleic acid, which cause inflammation and elevated cytokines, thus worsening lung, kidney injury, and shock culminating in multi-system organ failure and reduced survival. We additionally note that *PNLIP* has no role in the mechanisms leading to the initiation of acute pancreatitis or the signaling mediated by the lipotoxic NEFAs such as linoleic acid (LA) generated by lipolysis. Remarkably, this cascade of events leading to organ failure is independent of the principal adipocyte lipase, ATGL, which is present in diverticulitis but not pancreatitis.

Previous studies have shown that lipotoxic NEFA enriched in necrotic pancreatic fluid collections can cause mitochondrial damage, noted as swelling and disorganization of their ultrastructure, along with inhibiting complexes I and V (14). The systemic injury we note as TUNEL positive cells in the lungs and kidneys has previously been shown using oleic acid (21, 23, 24) and linoleic acid (40, 68), and during human ARDS (51). Here we identify PNLIP as the principal lipase mediating this uncontrolled generation of NEFA from visceral fat lipolysis.

While visceral adipose stranding is radiologically seen around the affected tissue during acute pancreatitis, appendicitis, acute diverticulitis (69), epiploic appendicitis, and omental infarction(1, 2), its role in predicting severity has only been noted in acute pancreatitis (5-7). This study shows PNLIP mediates this severity by hydrolyzing visceral fat during acute pancreatitis but not acute diverticulitis, despite the latter having intense inflammation (Fig. 1E). This pathophysiology is evidenced by **1)** triglycerides being the predominant lipid class in the fat of acute diverticulitis, but NEFA being the one in acute pancreatitis (Fig. 1M); **2)** Histological evidence of PNLIP in fat necrosis (Fig. 1L); **3)** Biochemical evidence of PNLIP in fat necrosis (Fig. 7B, C, S2B); **4)** Histologic areas positive for PNLIP staining positive for calcium on von-Kossa (Figs. 1C, S6) signifying saponified NEFAs; **5)** Pancreatic lipase injection into visceral fat causing fat necrosis (Fig. 2B) and generating large amounts of NEFA (Fig. 2D, E), resulting in systemic inflammation and organ failure (Fig. 2F-K); **6)** Oleic acid which is generated in this fat necrosis, alone being able to induce systemic inflammation and organ failure (Fig. 3A-H); **7)** The

levels of oleic acid noted in the serum of mice with organ failure being the same as patients with pancreatitis who have organ failure (Fig. 3A, I); and lastly **8)** The *in vitro* cellular models (Figs. 4, 5) and mechanistically distinct mouse pancreatitis models (Figs. 6, 7, S11) showing that genetic deletion of *PNLIP* protects from lipotoxic local and systemic injury.

The mechanism underlying the reduction in adipocyte proteins including ATGL and perilipin-1 in acute pancreatitis associated fat necrosis (Figs. 1Q, S2B, S2K) remains unclear. Trypsin is produced in the pancreas, and we note it to be present in fat necrosis (Figs. 1P, S2L) along with PNLIP and amylase. Trypsin can degrade ATGL (53), which may explain ATGL reduction in the fat during severe necrotizing pancreatitis (Figs. 1Q, 7C, S2B). This finding, along with acute pancreatitis associated fat necrosis in *ATGL* KO mice having increased PNLIP resulting in high cytokines, serum NEFA increase, and organ failure (Fig. 7), supports these outcomes to be independent of ATGL. This is further supported by the co-culture system in which we note adipocyte induced acinar injury to be dependent on lipolysis (since it is inhibited by orlistat, and in *PNLIP* KO mice acini), which is unaffected by using atiglistatin or *ATGL* KO adipocytes (Fig 4). Therefore, while ATGL does play a major role in regulated lipolysis of adipocyte triglyceride such as due to isoproterenol (Fig. S5), its role in acute pancreatitis associated visceral adipose tissue necrosis and organ failure is unlikely.

Among the pancreatic lipases, we note that PNLIP, which contributes to 80-90% of the pancreas' lipolytic activity, has a bigger role than PNLIPRP2 (Fig. 5A-E) in lipotoxic cell injury due to the hydrolysis of triglyceride. This relative abundance of PNLIP can explain the protective phenotype we observe *in vitro* (Fig. 5F-I) and *in vivo* (Figs. 6, 7, S11). The role of another lipase is possible, noting the minimal fat necrosis in the *PNLIP* KO mice during IL12, 18 acute pancreatitis (Fig. S11D), and partial protection from GTL induced injury in acini from the *PNLIP* KO mice (Fig. 5F, G). However, PNLIPRP2's clinical relevance is likely to be low since about 50% of Europeans are heterozygous and 20% homozygous for a common PNLIPRP2 truncation variant which results in nonsense-mediated decay, thus inhibiting expression of

PNLIPRP2 on the mRNA level (70). Since carboxyl ester lipase cannot effectively hydrolyze triglycerides with fatty acids of >16 carbon chains (38, 39) and requires bile acid concentrations much higher than in pancreatic necrosis collections (40), it is unlikely to play a major role in fat necrosis.

The protection afforded in the *PNLIP* KO acini and in mice is unique since *PNLIP* does not interfere with the mechanisms initiating pancreatitis such as the caerulein induced increase in cytosolic calcium or trypsinogen activation (Fig. 8A, C). This supports the hypothesis that inhibiting or neutralizing a disease modifier (in this case PNLIP) can change disease outcomes even after disease initiation. This finding also allows PNLIP neutralization or inhibition to be a therapeutic strategy, since fat necrosis becomes visible after 12 hours of pancreatitis (Fig. S2A) and precedes organ failure (Fig. S2I).

The data from the randomly accrued series of human samples, while blinded are limited by the study design being observational, small in size, and us not controlling for the use of intravenous lipids. Despite these limitations, the differences between diverticulitis and pancreatitis outcomes are significant. Future studies to validate these may be helpful. In the mouse studies, the small group size (3-7) for each sex, may have limited our ability to detect such differences. We also do not focus on the other factors that may influence PNLIP action. For example, we do not detail amount or type of phospholipase(s) or the dose response and time course of PNLIPRP2 that allow PNLIP entry into adipocytes (Fig. S4). Similarly, we did not study the role of co-lipase, which is PNLIP's co-factor that increases its activity 3-5 fold (26). Additionally, while adiponectin was detectable, ATGL or perilipin-1 underwent proteolysis. This is potentially explained by progressive accumulation of trypsin during fat necrosis in murine acute pancreatitis (Fig. S2L), and the detectable trypsin activity (Fig. 1P) in human acute pancreatitis-associated visceral adipose tissue necrosis. Overall, the genetic and pharmacologic evidence provided make PNLIP and not ATGL the likely mediator of the acute visceral adipose tissue lipolysis which worsens acute pancreatitis.

In summary, we note PNLIP, but not ATGL to be the principal mediator of excessive and unregulated visceral adipose tissue lipolysis during acute pancreatitis. This phenomenon does not take place in diverticulitis and explains why the visceral adipose tissue involvement in acute pancreatitis parallels disease severity. This also explains the prognostic role of visceral adipose tissue involvement in acute pancreatitis but not diverticulitis and perhaps other acute abdominal diseases. Visceral adipose tissue lipolysis by PNLIP generates a large amount of NEFA, which mediate severity of acute pancreatitis independent of its initiation, potentially making PNLIP a pharmacologic target to improve outcomes after disease onset.

Methods:

Human samples: All human studies were approved by the institutional review board of the Mayo Clinic (16-000973), University of Pittsburgh (Pro00000496) or Committee for Oversight of Research Involving the Dead University of Pittsburgh. We compared acute diverticulitis to acute pancreatitis for the following reasons: A) both are acute, B) both occur in the same demographic, C) both have radiographic (e.g., CT scans) and pathologic involvement of visceral fat, yet 4) their outcomes are very different, with a high prevalence of organ failure in pancreatitis versus diverticulitis. We wanted to understand the mechanism of higher organ failure in pancreatitis. All biochemical studies (October 2015 till May 2017) were done as part of a prospectively done observational study using consecutively procured patient waste residual samples remaining after drainage or after testing and processing had been completed on the tissue (in the pathology or microbiology departments) for medically indicated procedures independent of this research, and the residual was ready to be discarded. For example, the samples used for the current studies were residual material from pancreatic necrosis drained as per the revised Atlanta criteria (52) via surgical, endoscopic, or percutaneous debridement. The debridement procedures were clinically indicated and we had no control over what surgery the patient had, or which sample was designated as waste. These specimens were de-identified by

an honest broker and the analysts were blinded to the patients' clinical data till after all biochemical analyses and histological analyses were complete. Histology was done on formalin fixed paraffin embedded samples of surgically resected tissue (diverticulitis) of the same patients whose samples were analyzed biochemically (n=8), or acute pancreatitis sections (n=8) retrieved from an autopsy database search described in a previous study (14) while excluding autolysis and post mortem change as described therein (14). Transportation from the clinical source to the research lab was within 30 minutes of being released. These were kept on ice, aliquoted, and then frozen at -80C or fixed in formalin. Once 8 samples from each group had been procured and analyzed, the clinical data were mined. Organ failure was defined by a modified Marshall score of ≥ 2 more for the respiratory, renal or cardiovascular system, which is used to stratify patients in by the revised Atlanta criteria (52).

University of Pittsburgh severe acute pancreatitis patient cohort: This cohort was used to compare the serum levels of oleic acid in humans with severe acute pancreatitis to the mice with organ failure in a blinded and independent fashion. Samples were from the Pancreatitis-associated Risk of Organ Failure (PROOF) study. PROOF is an observational study at UPMC of subjects with AP early in their hospitalization, which recently completed enrollment. The PROOF protocol has been approved by the Institutional Review Board (IRB) of the University of Pittsburgh (Pro00000496) and submitted to the US National Library of Medicine (ClinicalTrials.gov Identifier: NCT03075605). The clinical protocol and cohort characteristics have been previously described (71). For this analysis, serum samples of 15 randomly chosen patients with severe AP patients and demographically matched controls without pancreatic diseases enrolled in PROOF between 2012 and 2015 were collected at enrollment and subsequent days when available. Oleic acid was extracted and quantitated using gas chromatography separation with flame ionization detection as previously described (72). Data on demographics, etiology, and clinical course were prospectively collected. Severity was defined by the Revised Atlanta Classification (52).

Mice Studies:

Genetic background: C57BL/6J wild type (WT) mice, mice with a targeted null allele of *Pnlip* [*PNLIP* KO mice; B6.129(Cg)-*Pnlip*^{tm1Dyh}/J, Jax Stock #008884] congenic on C57BL/6J (originally generated by Huggins et al.) (37), and mice with the null *Lep*^{ob} allele of leptin (wt/ob or ob/ob mice; B6.Cg-*Lep*^{ob}/J, Jax Stock #00632) congenic on C57BL/6J were obtained from the Jackson Laboratory (Bar Harbor, ME) and mated as described below. Mice with a LoxP-modified *Atgl*/*Pnpla2* allele (*Atgl*^{flox}mice; B6N.129S-*Pnpla2*^{tm1Eek}/J, Jax Stock #24278, originally generated by Sitnick et al. (36)) and mice expressing Cre recombinase under the control of the adipocyte-specific *Adipoq* promoter (Adipoq-cre mice (73); B6;FVB-Tg(*Adipoq*-cre)^{1Evdr}/J, Jax Stock #010803) were likewise obtained from the Jackson Laboratory. *Atgl*^{flox}mice and *Adipoq*-cre mice were mated to generate adipocyte-specific *ATGL* knockout mice (*ATGL* KO) (30) and subsequently made congenic on C57BL/6Ntac. To generate *PNLIP* and *ATGL* KO mice with genetic obesity due to leptin mutation the breeding schemes in supplementary Figures 13 and 14 respectively were used. *PNLIP* KO and *ATGL* KO mice were serially mated to leptin heterozygous (wt/ob) mice for at least 2 generations with selection of the desired alleles to generate experimental mice in the following groups: 1) ob/ob *PNLIP* KO, which were homozygous for both leptin (ob/ob) and *PNLIP* KO alleles congenic on C57BL/6J, and 2) ob/ob *ATGL* KO, which were homozygous for leptin and *ATGL*^{flox} alleles and heterozygous for the Cre allele. Although the latter were mixed C57BL/6J (>75%) and C57BL/6Ntac (<25%), confirmatory experiments revealed that these mice had loss of *ATGL* and its lipolytic action (Fig. 7C; Fig. S5) and were phenotypically similar to the other strains in the study (Fig. 6A, B). Obese littermates homozygous for leptin (ob/ob) with WT for *PNLIP* or *ATGL* were used as controls. Mice with a genetic deletion of PNLIPRP2 generated as described previously (74) were used to study its role in comparison to *PNLIP*. The genotype of all mice was confirmed after agarose gel electrophoresis of polymerase chain reaction amplification of tail DNA following Jackson Laboratory genotyping protocols and using AccuStart II PCR Genotyping Kit (Quantabio).

PNLIP KO mice were identified using the following primers: wild type forward - CAA ACA GCT AAT TAC TTC AGA TGC, KO forward - GCT ATC AGG ACA TAG CGT TGG, and common reverse - GGA CAG TGT CTT GCT GGT CTC, yielding a 380 bp band for *PNLIP* KO and a 185 bp band for wild type. Leptin deficient ob/ob mice were identified using three-primer mixes protocol (75) with subsequent confirmation by phenotypic weight gain. *ATGL*-flox mice were identified using the following primers: forward - ATC AGG CAG CCA CTC CAA C and reverse - GAG TGC AGT GTC CTT CAC CA, yielding a 390 bp band for *ATGL*-flox and a 235 bp band for wild type. Adipoq-cre were identified using the following primers: forward - ACG GAC AGA AGC ATT TTC CA, reverse - GGA TGT GCC ATG TGA GTC TG, yielding a 200 bp band for Cre.

Mice were housed in a temperature and humidity-controlled room with 12h light/dark cycle, with *ad libitum* access to standard chow (Purina 5053 diet, LabDiet, St. Louis, MO) and water. All animal protocols used in this study were approved by the Institutional Animal Care and Use Committee at Mayo Clinic. Males and females were used in this study.

Body weight and body composition assessment: Mouse weight, body fat and lean mass were analyzed by quantitative nuclear magnetic resonance (NMR) as previously (13) just before the experiments. Rest of the methods are described in the supplementary section.

Statistics: Independent variables for *in vivo* and *in vitro* studies are shown as bar graphs reported as mean ± SEM. line graphs were used for continuous variables. Significance levels were evaluated at $p<0.05$. Data for multiple groups were compared by 1-way ANOVA versus controls and values significantly different from controls were shown as (*) unless otherwise mentioned specifically in the legend (e.g., Fig. 2). When comparing 2 groups a t-test or Mann-Whitney test was used depending on the normality of distribution. Graphing was done using SigmaPlot 12.5 (Systat Software, Inc, San Jose, CA).

Study approvals: All animal protocols used in this study were approved by the Institutional Animal Care and Use Committee at Mayo Clinic. All human studies were approved by the institutional review board at the Mayo Clinic, or the University of Pittsburgh as detailed under the human studies section. Written informed consent from participants or their guardians was as per IRB protocol.

The rest of the methods are described in the supplementary section.

Author contributions: VPS designed, supervised and conceptualized the study. Acquisition, and analysis of data was facilitated and carried out by CDO, BK, PN, SK, AB, AEP, BB, KP, AG, MM, AM, DLH, SN, ST, DF, NF, RP, EK, ML, VPS while DLH, SN, DF, GIP, RP, EK, ML, VPS critically evaluated the manuscript. Interpretation of data was done by CDO, BK, PN, SK, AB, AEP, BB, DLH, GIP, SN, ML and VPS. Manuscript was drafted by CDO, BK, AB, SK, and VPS. Statistical analysis was done by CDO, BK, GIP, SK, BB and VPS. Funding was obtained by VPS. Order of first authorship was based on duration on project. "The authors have declared that no conflict of interest exists."

Acknowledgements: We would like to thank Mr. Michael King for the design of Figure 8. The help of the Mayo Clinic Scottsdale, BAP core, especially Ashley Droddy, Joshua Sandolo, Darin Posey is greatly appreciated in the efficient procurement and cataloging of the patient samples used in this study. This project was supported by the following fundings: R01DK092460, R01DK119646 from the NIDDK and PR151612 from the DOD (VPS); R01 R01DK090166 (EEK).

References:

1. Pereira JM, Sirlin CB, Pinto PS, Jeffrey RB, Stella DL, and Casola G. Disproportionate fat stranding: a helpful CT sign in patients with acute abdominal pain. *Radiographics.* 2004;24(3):703-15.
2. Tonerini M, Calcagni F, Lorenzi S, Scalise P, Grigolini A, and Bemi P. Omental infarction and its mimics: imaging features of acute abdominal conditions presenting with fat stranding greater than the degree of bowel wall thickening. *Emerg Radiol.* 2015.
3. Avanesov M, Wiese NJ, Karul M, Guerreiro H, Keller S, Busch P, et al. Diagnostic prediction of complicated appendicitis by combined clinical and radiological appendicitis severity index (APSI). *Eur Radiol.* 2018;28(9):3601-10.
4. Kim HY, Park JH, Lee YJ, Lee SS, Jeon JJ, and Lee KH. Systematic Review and Meta-Analysis of CT Features for Differentiating Complicated and Uncomplicated Appendicitis. *Radiology.* 2018;287(1):104-15.
5. Balthazar EJ, Robinson DL, Megibow AJ, and Ranson JH. Acute pancreatitis: value of CT in establishing prognosis. *Radiology.* 1990;174(2):331-6.
6. Meyrignac O, Lagarde S, Bournet B, Mokrane FZ, Buscail L, Rousseau H, et al. Acute Pancreatitis: Extrapancreatic Necrosis Volume as Early Predictor of Severity. *Radiology.* 2015:141494.
7. Bollen TL, Singh VK, Maurer R, Repas K, van Es HW, Banks PA, et al. A comparative evaluation of radiologic and clinical scoring systems in the early prediction of severity in acute pancreatitis. *Am J Gastroenterol.* 2012;107(4):612-9.
8. Cirocchi R, Randolph JJ, Binda GA, Gioia S, Henry BM, Tomaszewski KA, et al. Is the outpatient management of acute diverticulitis safe and effective? A systematic review and meta-analysis. *Tech Coloproctol.* 2019;23(2):87-100.
9. Garg PK, and Singh VP. Organ Failure Due to Systemic Injury in Acute Pancreatitis. *Gastroenterology.* 2019;156(7):2008-23.
10. Sennello JA, Fayad R, Pini M, Gove ME, Ponemone V, Cabay RJ, et al. Interleukin-18, together with interleukin-12, induces severe acute pancreatitis in obese but not in nonobese leptin-deficient mice. *Proc Natl Acad Sci U S A.* 2008;105(23):8085-90.
11. Zyromski NJ, Mathur A, Pitt HA, Lu D, Gripe JT, Walker JJ, et al. A murine model of obesity implicates the adipokine milieu in the pathogenesis of severe acute pancreatitis. *Am J Physiol Gastrointest Liver Physiol.* 2008;295(3):G552-8.
12. Misumi I, Starmer J, Uchimura T, Beck MA, Magnuson T, and Whitmire JK. Obesity Expands a Distinct Population of T Cells in Adipose Tissue and Increases Vulnerability to Infection. *Cell Rep.* 2019;27(2):514-24 e5.
13. Patel K, Trivedi RN, Durgampudi C, Noel P, Cline RA, DeLany JP, et al. Lipolysis of visceral adipocyte triglyceride by pancreatic lipases converts mild acute pancreatitis to severe pancreatitis independent of necrosis and inflammation. *Am J Pathol.* 2015;185(3):808-19.
14. Navina S, Acharya C, DeLany JP, Orlichenko LS, Baty CJ, Shiva SS, et al. Lipotoxicity causes multisystem organ failure and exacerbates acute pancreatitis in obesity. *Sci Transl Med.* 2011;3(107):107ra10.
15. Tschop J, Nogueiras R, Haas-Lockie S, Kasten KR, Castaneda TR, Huber N, et al. CNS leptin action modulates immune response and survival in sepsis. *J Neurosci.* 2010;30(17):6036-47.
16. Shapiro NI, Khankin EV, Van Meurs M, Shih SC, Lu S, Yano M, et al. Leptin exacerbates sepsis-mediated morbidity and mortality. *J Immunol.* 2010;185(1):517-24.
17. Niiyama S, Takasu O, Sakamoto T, and Ushijima K. Intraperitoneal adipose tissue is strongly related to survival rate in a mouse cecal ligation and puncture model. *Clin Transl Immunology.* 2016;5(2):e64.

18. Domschke S, Malfertheiner P, Uhl W, Buchler M, and Domschke W. Free fatty acids in serum of patients with acute necrotizing or edematous pancreatitis. *Int J Pancreatol.* 1993;13(2):105-10.
19. Sztefko K, and Panek J. Serum free fatty acid concentration in patients with acute pancreatitis. *Pancreatology.* 2001;1(3):230-6.
20. Durgampudi C, Noel P, Patel K, Cline R, Trivedi RN, DeLany JP, et al. Acute Lipotoxicity Regulates Severity of Biliary Acute Pancreatitis without Affecting Its Initiation. *Am J Pathol.* 2014;184(6):1773-84.
21. Wu RP, Liang XB, Guo H, Zhou XS, Zhao L, Wang C, et al. Protective effect of low potassium dextran solution on acute kidney injury following acute lung injury induced by oleic acid in piglets. *Chin Med J (Engl).* 2012;125(17):3093-7.
22. Dettelbach MA, Deftos LJ, and Stewart AF. Intraperitoneal free fatty acids induce severe hypocalcemia in rats: a model for the hypocalcemia of pancreatitis. *J Bone Miner Res.* 1990;5(12):1249-55.
23. Lai JP, Bao S, Davis IC, and Knoell DL. Inhibition of the phosphatase PTEN protects mice against oleic acid-induced acute lung injury. *Br J Pharmacol.* 2009;156(1):189-200.
24. Hussain N, Wu F, Zhu L, Thrall RS, and Kresch MJ. Neutrophil apoptosis during the development and resolution of oleic acid-induced acute lung injury in the rat. *Am J Respir Cell Mol Biol.* 1998;19(6):867-74.
25. Wang S, Soni KG, Semache M, Casavant S, Fortier M, Pan L, et al. Lipolysis and the integrated physiology of lipid energy metabolism. *Mol Genet Metab.* 2008;95(3):117-26.
26. Giller T, Buchwald P, Blum-Kaelin D, and Hunziker W. Two novel human pancreatic lipase related proteins, hPLRP1 and hPLRP2. Differences in colipase dependence and in lipase activity. *J Biol Chem.* 1992;267(23):16509-16.
27. De Caro J, Sias B, Grandval P, Ferrato F, Halimi H, Carriere F, et al. Characterization of pancreatic lipase-related protein 2 isolated from human pancreatic juice. *Biochim Biophys Acta.* 2004;1701(1-2):89-99.
28. Lowe ME. The triglyceride lipases of the pancreas. *J Lipid Res.* 2002;43(12):2007-16.
29. Schreiber R, Xie H, and Schweiger M. Of mice and men: The physiological role of adipose triglyceride lipase (ATGL). *Biochim Biophys Acta Mol Cell Biol Lipids.* 2018.
30. Schoiswohl G, Stefanovic-Racic M, Menke MN, Wills RC, Surlow BA, Basantani MK, et al. Impact of Reduced ATGL-Mediated Adipocyte Lipolysis on Obesity-Associated Insulin Resistance and Inflammation in Male Mice. *Endocrinology.* 2015;156(10):3610-24.
31. Parajuli N, Takahara S, Matsumura N, Kim TT, Ferdaoussi M, Migglautsch AK, et al. Atglistatin ameliorates functional decline in heart failure via adipocyte-specific inhibition of adipose triglyceride lipase. *Am J Physiol Heart Circ Physiol.* 2018;315(4):H879-H84.
32. Prasada R, Dhaka N, Bahl A, Yadav TD, and Kochhar R. Prevalence of cardiovascular dysfunction and its association with outcome in patients with acute pancreatitis. *Indian J Gastroenterol.* 2018;37(2):113-9.
33. Halonen KI, Pettila V, Leppaniemi AK, Kemppainen EA, Puolakkainen PA, and Haapiainen RK. Multiple organ dysfunction associated with severe acute pancreatitis. *Crit Care Med.* 2002;30(6):1274-9.
34. Noel P, Patel K, Durgampudi C, Trivedi RN, de Oliveira C, Crowell MD, et al. Peripancreatic fat necrosis worsens acute pancreatitis independent of pancreatic necrosis via unsaturated fatty acids increased in human pancreatic necrosis collections. *Gut.* 2014.
35. Mayer N, Schweiger M, Romauch M, Grabner GF, Eichmann TO, Fuchs E, et al. Development of small-molecule inhibitors targeting adipose triglyceride lipase. *Nat Chem Biol.* 2013;9:785.

36. Sitnick MT, Basantani MK, Cai L, Schoiswohl G, Yazbeck CF, Distefano G, et al. Skeletal muscle triacylglycerol hydrolysis does not influence metabolic complications of obesity. *Diabetes.* 2013;62(10):3350-61.
37. Huggins KW, Camarota LM, Howles PN, and Hui DY. Pancreatic triglyceride lipase deficiency minimally affects dietary fat absorption but dramatically decreases dietary cholesterol absorption in mice. *J Biol Chem.* 2003;278(44):42899-905.
38. Lombardo D, Fauvel J, and Guy O. Studies on the substrate specificity of a carboxyl ester hydrolase from human pancreatic juice. I. Action on carboxyl esters, glycerides and phospholipids. *Biochim Biophys Acta.* 1980;611(1):136-46.
39. Fontbonne H, Brisson L, Verine A, Puigserver A, Lombardo D, and Ajandouz el H. Human bile salt-dependent lipase efficiency on medium-chain acyl-containing substrates: control by sodium taurocholate. *J Biochem.* 2011;149(2):145-51.
40. Khatua B, Trivedi RN, Noel P, Patel K, Singh R, de Oliveira C, et al. Carboxyl Ester Lipase May Not Mediate Lipotoxic Injury during Severe Acute Pancreatitis. *Am J Pathol.* 2019.
41. Zhang Y, Proenca R, Maffei M, Barone M, Leopold L, and Friedman JM. Positional cloning of the mouse obese gene and its human homologue. *Nature.* 1994;372(6505):425-32.
42. Pini M, Sennello JA, Cabay RJ, and Fantuzzi G. Effect of diet-induced obesity on acute pancreatitis induced by administration of interleukin-12 plus interleukin-18 in mice. *Obesity (Silver Spring).* 2010;18(3):476-81.
43. Acharya C, Cline RA, Jaligama D, Noel P, Delany JP, Bae K, et al. Fibrosis Reduces Severity of Acute-on-Chronic Pancreatitis in Humans. *Gastroenterology.* 2013;145(2):466-75.
44. Aho HJ, Sternby B, and Nevalainen TJ. Fat necrosis in human acute pancreatitis. An immunohistological study. *Acta Pathol Microbiol Immunol Scand A.* 1986;94(2):101-5.
45. Aho HJ, Sternby B, Kallajoki M, and Nevalainen TJ. Carboxyl ester lipase in human tissues and in acute pancreatitis. *Int J Pancreatol.* 1989;5(2):123-34.
46. Kloppel G, Dreyer T, Willemer S, Kern HF, and Adler G. Human acute pancreatitis: its pathogenesis in the light of immunocytochemical and ultrastructural findings in acinar cells. *Virchows Arch A Pathol Anat Histopathol.* 1986;409(6):791-803.
47. Watanabe O, Baccino FM, Steer ML, and Meldolesi J. Supramaximal caerulein stimulation and ultrastructure of rat pancreatic acinar cell: early morphological changes during development of experimental pancreatitis. *Am J Physiol.* 1984;246(4 Pt 1):G457-67.
48. Gaisano HY, Lutz MP, Leser J, Sheu L, Lynch G, Tang L, et al. Supramaximal cholecystokinin displaces Munc18c from the pancreatic acinar basal surface, redirecting apical exocytosis to the basal membrane. *J Clin Invest.* 2001;108(11):1597-611.
49. Cosen-Binker LI, Lam PP, Binker MG, Reeve J, Pandol S, and Gaisano HY. Alcohol/cholecystokinin-evoked pancreatic acinar basolateral exocytosis is mediated by protein kinase C alpha phosphorylation of Munc18c. *J Biol Chem.* 2007;282(17):13047-58.
50. Liu X, Wang Y, Duclos RI, Jr., and O'Doherty GA. Stereochemical Structure Activity Relationship Studies (S-SAR) of Tetrahydrolipstatin. *ACS Med Chem Lett.* 2018;9(3):274-8.
51. Matthay MA, and Zemans RL. The acute respiratory distress syndrome: pathogenesis and treatment. *Annu Rev Pathol.* 2011;6:147-63.
52. Banks PA, Bollen TL, Dervenis C, Gooszen HG, Johnson CD, Sarr MG, et al. Classification of acute pancreatitis--2012: revision of the Atlanta classification and definitions by international consensus. *Gut.* 2013;62(1):102-11.
53. Xie X, Langlais P, Zhang X, Heckmann BL, Saarinen AM, Mandarino LJ, et al. Identification of a novel phosphorylation site in adipose triglyceride lipase as a regulator of lipid droplet localization. *Am J Physiol Endocrinol Metab.* 2014;306(12):E1449-59.

54. Nevalainen TJ, Eerola LI, Rintala E, Laine VJ, Lambeau G, and Gelb MH. Time-resolved fluoroimmunoassays of the complete set of secreted phospholipases A2 in human serum. *Biochim Biophys Acta.* 2005;1733(2-3):210-23.
55. Nevalainen TJ, Hietaranta AJ, and Gronroos JM. Phospholipase A2 in acute pancreatitis: new biochemical and pathological aspects. *Hepatogastroenterology.* 1999;46(29):2731-5.
56. Friess H, Shrikhande S, Riesle E, Kashiwagi M, Baczako K, Zimmermann A, et al. Phospholipase A2 isoforms in acute pancreatitis. *Ann Surg.* 2001;233(2):204-12.
57. Maleth J, Balazs A, Pallagi P, Balla Z, Kui B, Katona M, et al. Alcohol disrupts levels and function of the cystic fibrosis transmembrane conductance regulator to promote development of pancreatitis. *Gastroenterology.* 2015;148(2):427-39 e16.
58. van Dijk SM, Timmerhuis HC, Verdonk RC, Reijnders E, Bruno MJ, Fockens P, et al. Treatment of disrupted and disconnected pancreatic duct in necrotizing pancreatitis: A systematic review and meta-analysis. *Pancreatology.* 2019;19(7):905-15.
59. Patel K, Durgampudi C, Noel P, Trivedi RN, de Oliveira C, and Singh VP. Fatty Acid Ethyl Esters Are Less Toxic Than Their Parent Fatty Acids Generated during Acute Pancreatitis. *Am J Pathol.* 2016;186(4):874-84.
60. Panek J, Sztefko K, and Drozdz W. Composition of free fatty acid and triglyceride fractions in human necrotic pancreatic tissue. *Med Sci Monit.* 2001;7(5):894-8.
61. Ding L, Liou GY, Schmitt DM, Storz P, Zhang JS, and Billadeau DD. Glycogen synthase kinase-3beta ablation limits pancreatitis-induced acinar-to-ductal metaplasia. *J Pathol.* 2017;243(1):65-77.
62. Bhanot UK, and Moller P. Mechanisms of parenchymal injury and signaling pathways in ectatic ducts of chronic pancreatitis: implications for pancreatic carcinogenesis. *Lab Invest.* 2009;89(5):489-97.
63. Janiak A, Lesniowski B, Jasinska A, Pietruczuk M, and Malecka-Panas E. Interleukin 18 as an early marker or prognostic factor in acute pancreatitis. *Prz Gastroenterol.* 2015;10(4):203-7.
64. Wereszczynska-Siemiatkowska U, Mroczko B, and Siemiatkowski A. Serum profiles of interleukin-18 in different severity forms of human acute pancreatitis. *Scand J Gastroenterol.* 2002;37(9):1097-102.
65. Pandol SJ, Saluja AK, Imrie CW, and Banks PA. Acute pancreatitis: bench to the bedside. *Gastroenterology.* 2007;132(3):1127-51.
66. Williams JA, Sans MD, Tashiro M, Schafer C, Bragado MJ, and Dabrowski A. Cholecystokinin activates a variety of intracellular signal transduction mechanisms in rodent pancreatic acinar cells. *Pharmacol Toxicol.* 2002;91(6):297-303.
67. Williams JA. Intracellular signaling mechanisms activated by cholecystokinin-regulating synthesis and secretion of digestive enzymes in pancreatic acinar cells. *Annu Rev Physiol.* 2001;63:77-97.
68. de Oliveira C, Khatua B, Bag A, El-Kurdi B, Patel K, Mishra V, et al. Multimodal Transgastric Local Pancreatic Hypothermia Reduces Severity of Acute Pancreatitis in Rats and Increases Survival. *Gastroenterology.* 2019;156(3):735-47 e10.
69. Rao PM, and Rhea JT. Colonic diverticulitis: evaluation of the arrowhead sign and the inflamed diverticulum for CT diagnosis. *Radiology.* 1998;209(3):775-9.
70. Nemeth BC, Pesei ZG, Hegyi E, Szucs A, Szentesi A, Hegyi P, et al. The common truncation variant in pancreatic lipase related protein 2 (PNLIPRP2) is expressed poorly and does not alter risk for chronic pancreatitis. *PLoS One.* 2018;13(11):e0206869.
71. Mounzer R, Langmead CJ, Wu BU, Evans AC, Bishehsari F, Muddana V, et al. Comparison of existing clinical scoring systems to predict persistent organ failure in patients with acute pancreatitis. *Gastroenterology.* 2012;142(7):1476-82; quiz e15-6.

72. Kangani CO, Kelley DE, and Delany JP. New method for GC/FID and GC-C-IRMS analysis of plasma free fatty acid concentration and isotopic enrichment. *J Chromatogr B Analyt Technol Biomed Life Sci.* 2008;873(1):95-101.
73. Eguchi J, Wang X, Yu S, Kershaw EE, Chiu PC, Dushay J, et al. Transcriptional control of adipose lipid handling by IRF4. *Cell Metab.* 2011;13(3):249-59.
74. Lowe ME, Kaplan MH, Jackson-Grusby L, D'Agostino D, and Grusby MJ. Decreased neonatal dietary fat absorption and T cell cytotoxicity in pancreatic lipase-related protein 2-deficient mice. *J Biol Chem.* 1998;273(47):31215-21.
75. Ellett JD, Evans ZP, Zhang G, Chavin KD, and Spyropoulos DD. A rapid PCR-based method for the identification of ob mutant mice. *Obesity (Silver Spring).* 2009;17(2):402-4.

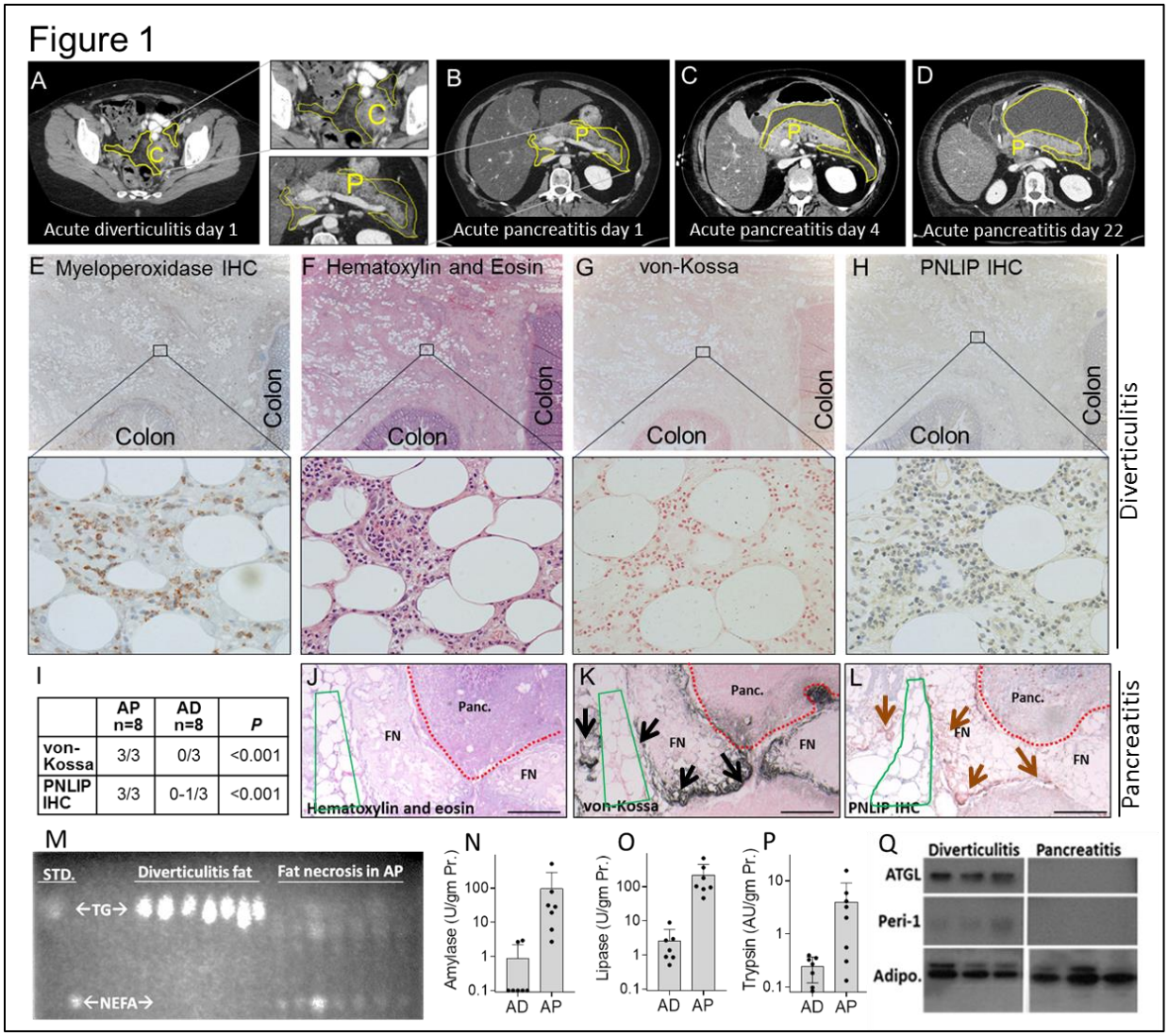

Figure 1: Comparison of biochemical parameters, histology of acute pancreatitis and diverticulitis in humans. Cross-sectional CT scan images on the first day of acute diverticulitis (**A**) or acute pancreatitis (**B-D**) with fat stranding of visceral adipose tissue (yellow outline) around the colon (C), or the pancreas (P). **B-D** show images depicting progression of visceral fat involvement (yellow line) on the different days after onset of pancreatitis mentioned at the bottom. A representative example of serial sections of human tissue stained for myeloperoxidase during acute diverticulitis (**E**) showing the colon on the right and lower edges of section, and magnified views of the insets below, of acute diverticulitis (**E-H**) and acute pancreatitis (**J-L**) stained for Hematoxylin & Eosin (**F, J**), calcium stain with von-Kossa (**G, K**), and IHC for PNLIP (**H, L**) are also shown. Note von-Kossa and PNLIP positive areas overlap (arrows) in areas of fat necrosis (FN), but not normal fat (green outline). Also note positive von-Kossa staining in necrosed pancreas (Panc) which has loss of cell outlines (above the dotted red line). This localizes the saponified NEFA in the necrosed pancreas. **I**: Table comparing von-Kossa and PNLIP positivity scores in acute pancreatitis (AP) and acute diverticulitis (AD) when read on a 0-3 scale, n=8. The *P* values (Student's t-test) show the significance of the difference **M:** Thin layer chromatography comparing the relative amount of NEFA with TG in samples from patients with acute pancreatitis or diverticulitis. Lipase (**N**), Amylase (**O**), and trypsin (**P**) activities measured in these samples**.** Error bars represent SEM. **Q:** Western blot images

comparing detectable ATGL and perilipin-1 (Peri-1), and adiponectin (Adipo) band in these samples.

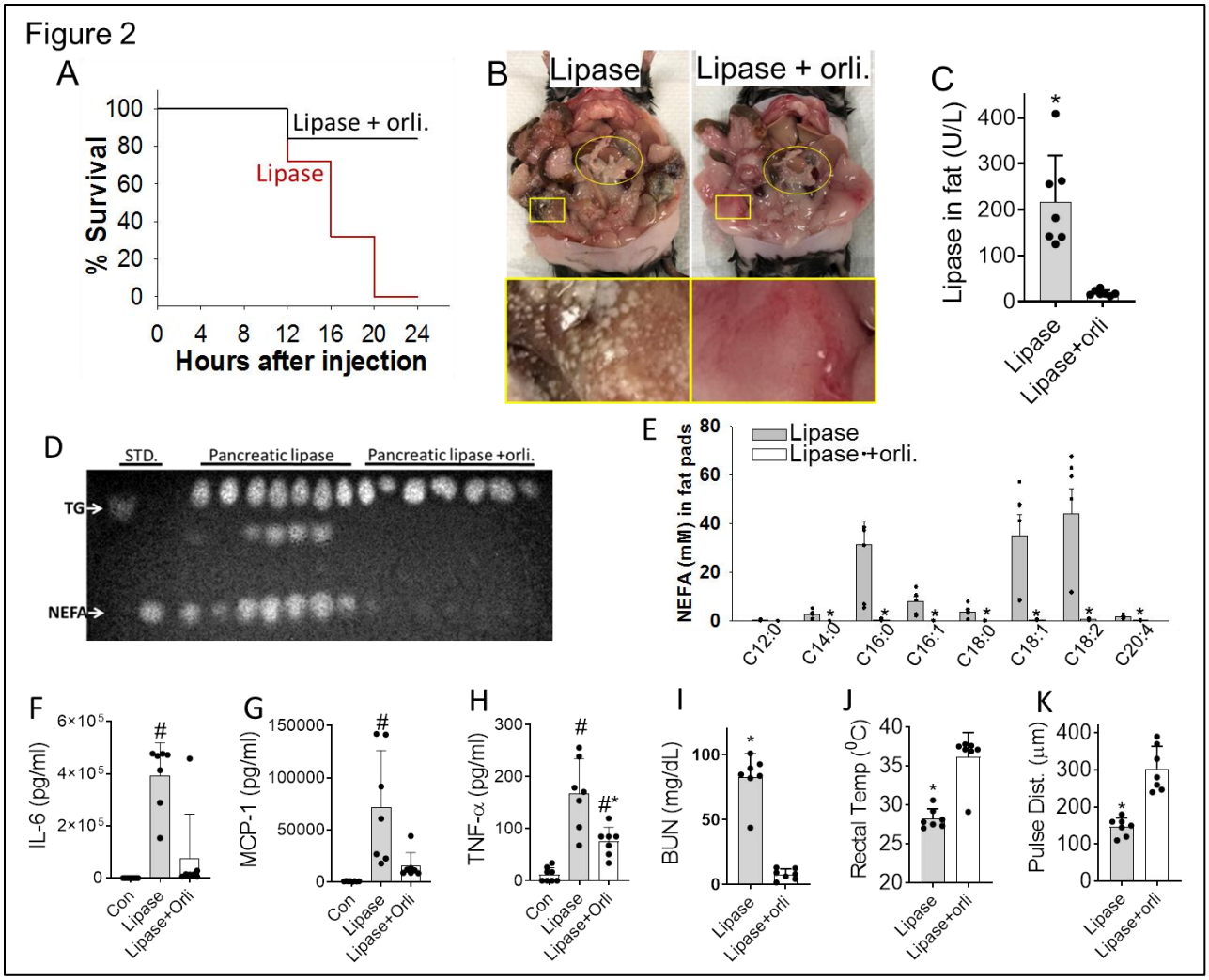

Figure 2: Effect of visceral fat lipolysis by pancreatic lipase injection in ob/ob mice without pancreatitis. A: Survival curves of the mice given lipase alone (red) or the lipase along with the lipase inhibitor orlistat (Lipase+orli**;** black line). **B:** Gross appearance of the pancreas (yellow oval) and visceral fat (Yellow rectangle) *in situ* at the time of necropsy. **C:** Pancreatic lipase activity in the gonadal fat pads of these mice at the time of necropsy. **D:** Thin layer chromatography comparing the relative amount of NEFA with TG in these fat pads. STD.: Standards. TG: glyceryl trioleate, triglyceride standard. NEFA; oleic acid, a NEFA standard. **E**: individual NEFA concentrations in the fat pads of the mice as measured by gas chromatography. **F-H:** Serum cytokines at the time of necropsy in controls (Con) and other groups mentioned below the respective bars. **I:** Serum BUN measured at the time of necropsy, and rectal temperature (**J),** and carotid pulse distention (pulse dist. **K**) measured in the lipase treated group at the last monitoring time before necropsy (12-16 hours after first injection) or in the orlistat group after 24 hours, and just before elective euthanasia. # indicates significant increase over untreated controls, and * indicates a significant difference between the lipase and Lipase+orli. groups based on a p value <0.05. Error bars represent SD.There were 7 mice per group.

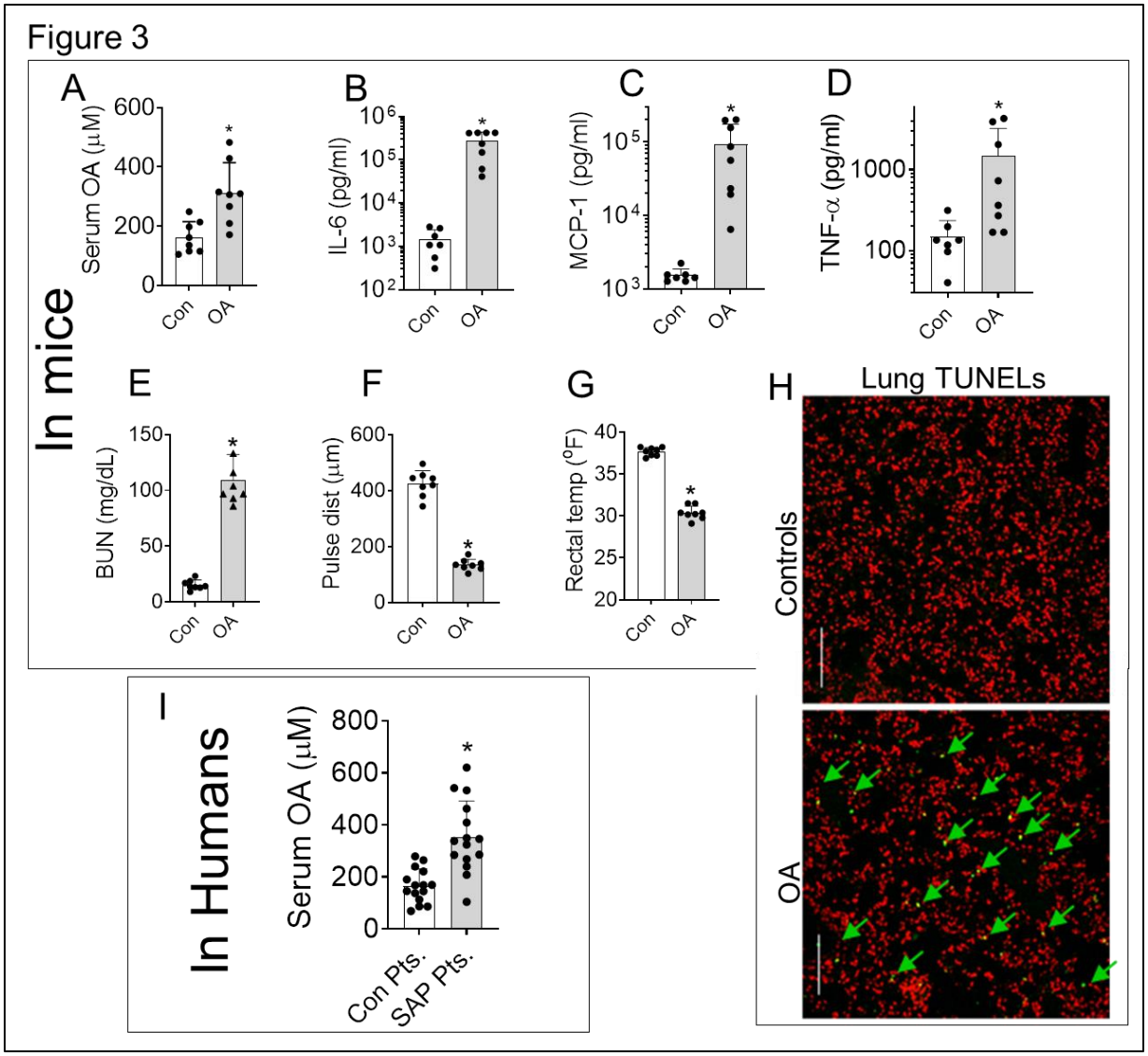

Figure 3: Relevance of oleic acid to systemic injury in mice and during human severe pancreatitis. A-E: Blood levels of serum oleic acid (OA; **A**), IL-6 **(B),** MCP-1 **(C)**, TNF-α (**D**), and BUN (**E**) in the control (Con) and OA treated groups of mice at the time of euthanasia. **F:** Carotid pulse distention and, **G:** Rectal temperatures prior to euthanasia of these mice. **H:** Representative images from lung histologic sections stained for TUNEL (green) with nuclei stained red. Arrows point to the positive staining nuclei. There were 8 mice in each group. **I:** Serum oleic acid levels in the control patient group (Con Pts.) and severe acute pancreatitis (SAP) patients from the PROOF cohort. * indicates a significant difference (P<0.05) between the two groups.Error bars represent SD.

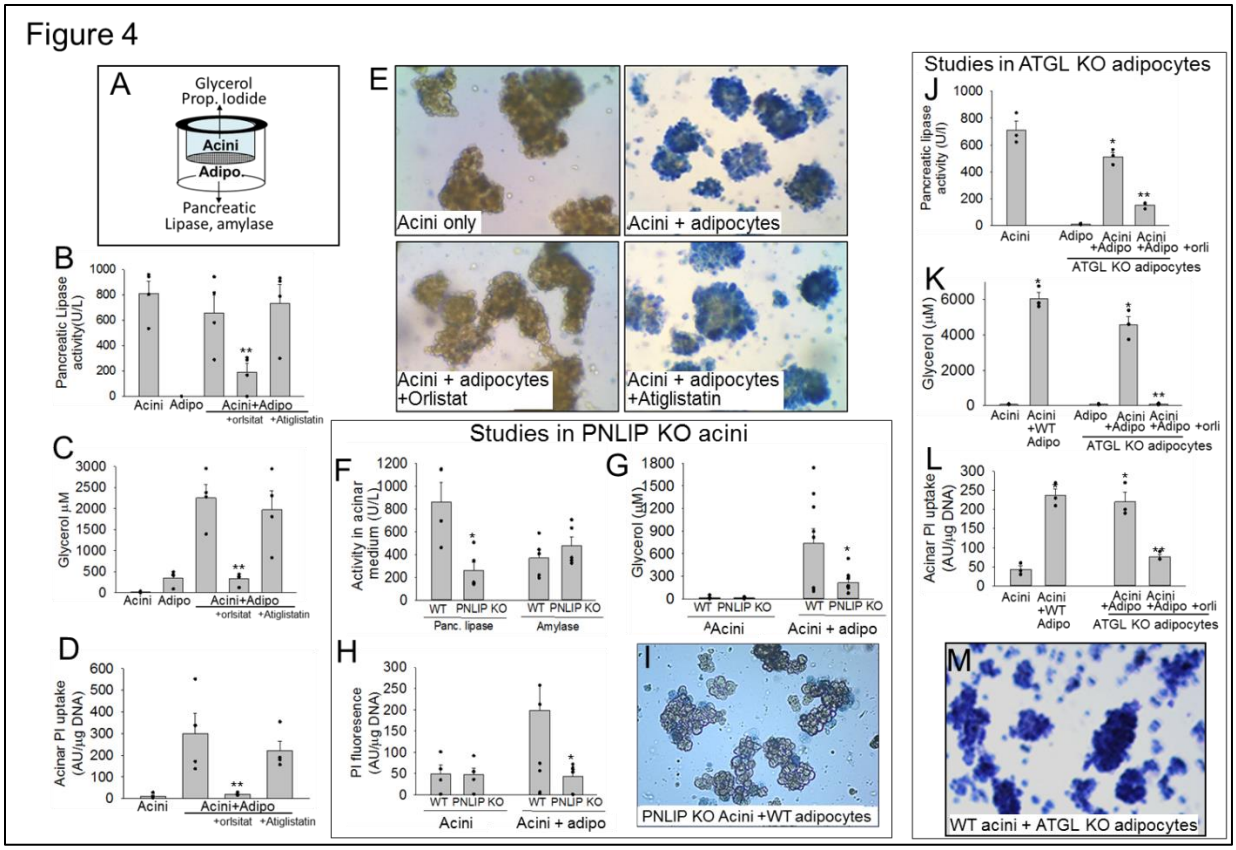

Figure 4: Comparison of pharmacologic or genetic inhibition of ATGL or PNLIP on adipocyte induced acinar injury: A: Schematic showing the setup of the pancreatic acini, adipocyte co-culture experiment using a transwell system with a 3µm mesh separating the acini from the adipocytes. **B-E**: Effect of the generic lipase inhibitor orlistat (50µM) and the ATGL specific inhibitor Atiglistatin (50µM) on the pancreatic lipase activity in the medium (**B**), glycerol generation in the medium, (**C**) and propidium iodide uptake (**D**), trypan blue staining (**E**) of pancreatic acini at the end of 6 hours of co-culture. **F:** Activity of pancreatic lipase and amylase in the media from acini of wild type (WT) or *PNLIP* KO mice. Effect of co-culturing acini from WT and *PNLIP* KO mice with WT adipocytes on glycerol generation (**G**) propidium iodide uptake (**H**) and trypan blue staining (**I**) of acini at the end of 6 hours of co-culture. Effect of culturing WT acini alone, with WT adipocytes or *ATGL* KO adipocytes (+/- orlistat; orli, 50µM) on the measurable pancreatic lipase activity in the medium (**J**), glycerol concentration in the medium (**K**), propidium iodide uptake (**L**) and trypan blue staining (**M)** by the acini. Each experiment was done 3-7 times separately. Each point represents a different experiment. *Indicates a signfincat change compared to other conditions in the group on ANOVA. ** indicates a selective reduction with orlistat (but not atilgistatin or deletion of ATGL as may be relevant to the experimental design). Error bars represent SEM.

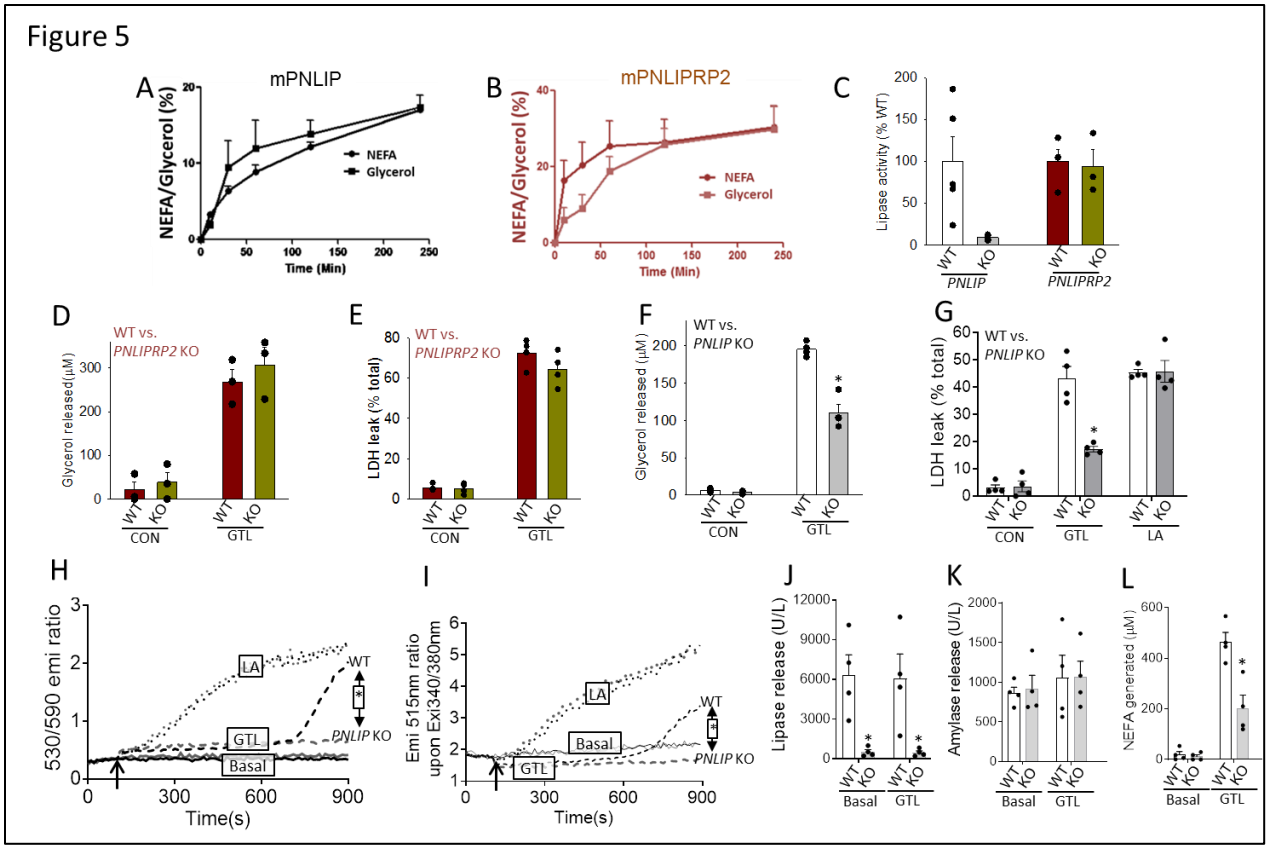

Figure 5: Comparison of lipolysis by PNLIP and PNLIPRP2, and their roles in acinar injury due to triglyceride lipolysis or direct fatty acid lipotoxicity. NEFA and glycerol generation from hydrolysis of glyceryl trilinoleate (GTL; 300μM) by recombinant murine PNLIP (**A**) and PNLIPRP2 (**B**) each at 1μg/ml. The Y axis is labelled with 100% lipolysis signifying complete lipolysis of the added GTL (300μM) generating 300μM glycerol or 900 μM of fatty acid. **C:** comparison of pancreatic lipase activity/tissue weight in homogenates of *PNLIP* KO (grey) or *PNLIPRP2* knockout (dirty yellow) mice vs. their wild type litter mates (white and burgundy respectively). Bar graphs showing the effect of incubating acini from wild type mice, or *PNLIPRP2* knockout mice on glycerol concentrations (**D, F**) and LDH leakage (**E, G**) in the medium. CON implies under control state without added GTL, and "GTL" implies after incubating with 300μM GTL for 2 hours. "LA" implies 600μM linoleic acid. **H-L:** Representative graphs comparing mitochondrial depolarization using JC-1 (**H**), cytosolic calcium increase using Fura-2AM (**I**) in WT and *PNLIP* KO acini, and the lipase (**J**), amylase (**K**) release, NEFA present (**L**) at the end of the 15 minute incubation in the medium of the respective cuvettes. * indicates a p <0.05 between the two groups. Each experiment was done 3-5 times separately.
Error bars represent SEM.

Figure 6

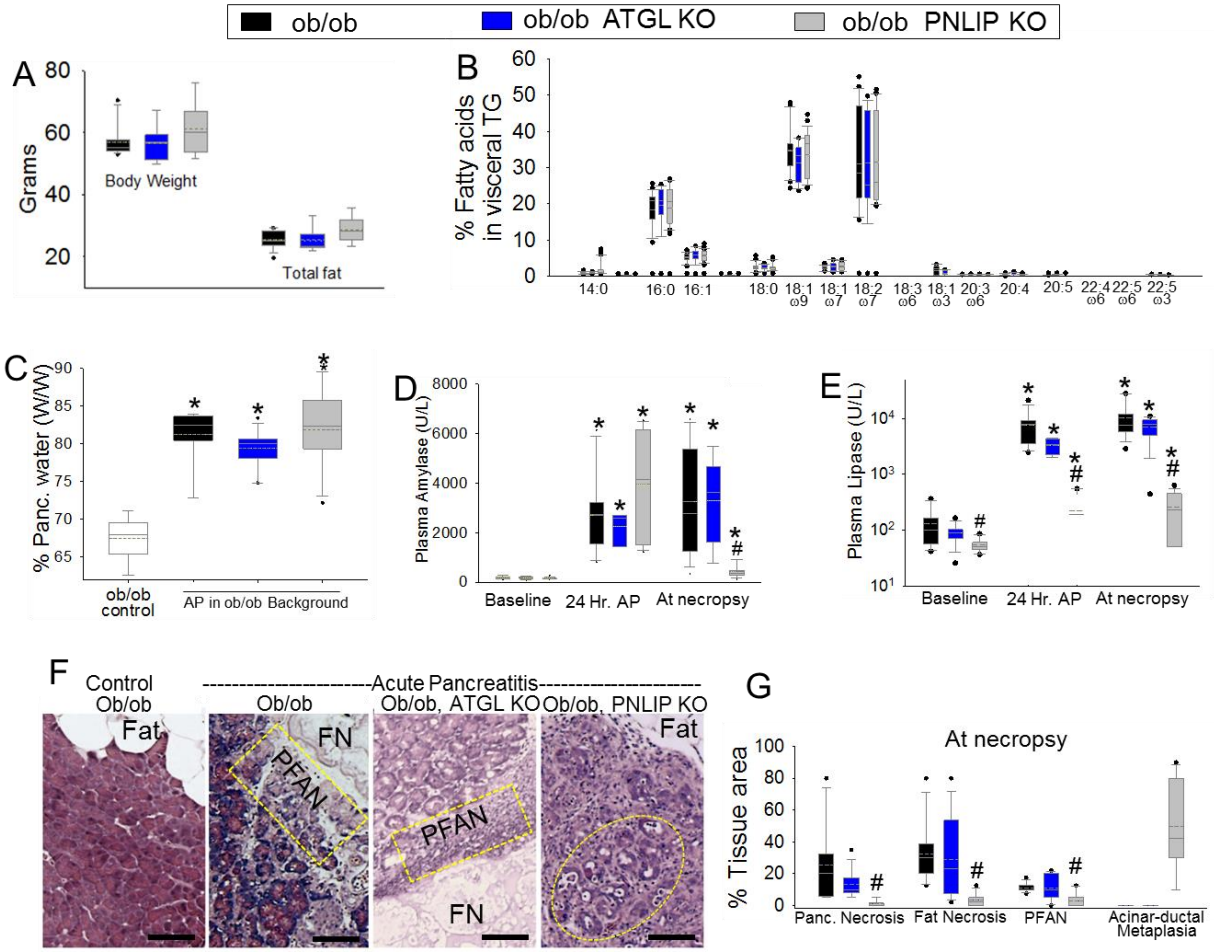

Figure 6: Parameters of obesity and caerulein acute pancreatitis in genetically obese littermate (ob/ob; black) mice, ob/ob mice with genetically deleted *ATGL* (*ATGL* KO; blue), or ob/ob mice with genetically deleted PNILP (*PNLIP* KO; grey). A: body weight and total fat content of the mice at baseline. **B:** NEFA composing visceral triglyceride. **C**: pancreatic edema (% water content in wet weight of the pancreas), in control mice (CON) and those with acute pancreatitis (AP). Serum amylase (**D**), and lipase (**E**) levels at baseline, 24 hours after pancreatitis and after euthanasia in the three strains of mice. **F**: hematoxylin and eosin staining of pancreas and surrounding fat. Note the presence of fat necrosis (FN) in the ob/ob, ob/ob, *ATGL* KO mice with acute pancreatitis. This is adjacent to the pancreas, which is severely damaged (peri-fat acinar necrosis; PFAN, shown in dashed yellow rectangles). The non-necrosed fat is listed as "fat". Dashed yellow oval in the ob/ob *PNLIP* KO mouse panel highlights the dilated lumens of the acini (acinar-ductal metaplasia), consistent with the chronic caerulein hyper-stimulation over the 5 days. The scale bars at the bottom measure 75μm **G**: Box plots comparing the areas of pancreatic necrosis, fat necrosis, PFAN and acinar ductal metaplasia in the 3 groups with pancreatitis. Box plots depict mean (dashed line), median (solid line), 25th and 75th percentiles (2 boxes), 10th and 90th percentiles (whiskers), and outliers (dots). **J**: Kidney TUNEL staining (brown nuclei, arros highlight some) ofthe various groups. * indicates a significant increase over controls or baseline from the same genetic group without pancreatitis on ANOVA. # indicates a significant difference in the *PNLIP* KO mice vs. other genetic background littermate mice in the same group of pancreatitis on ANOVA. Each group had 8-10 mice.

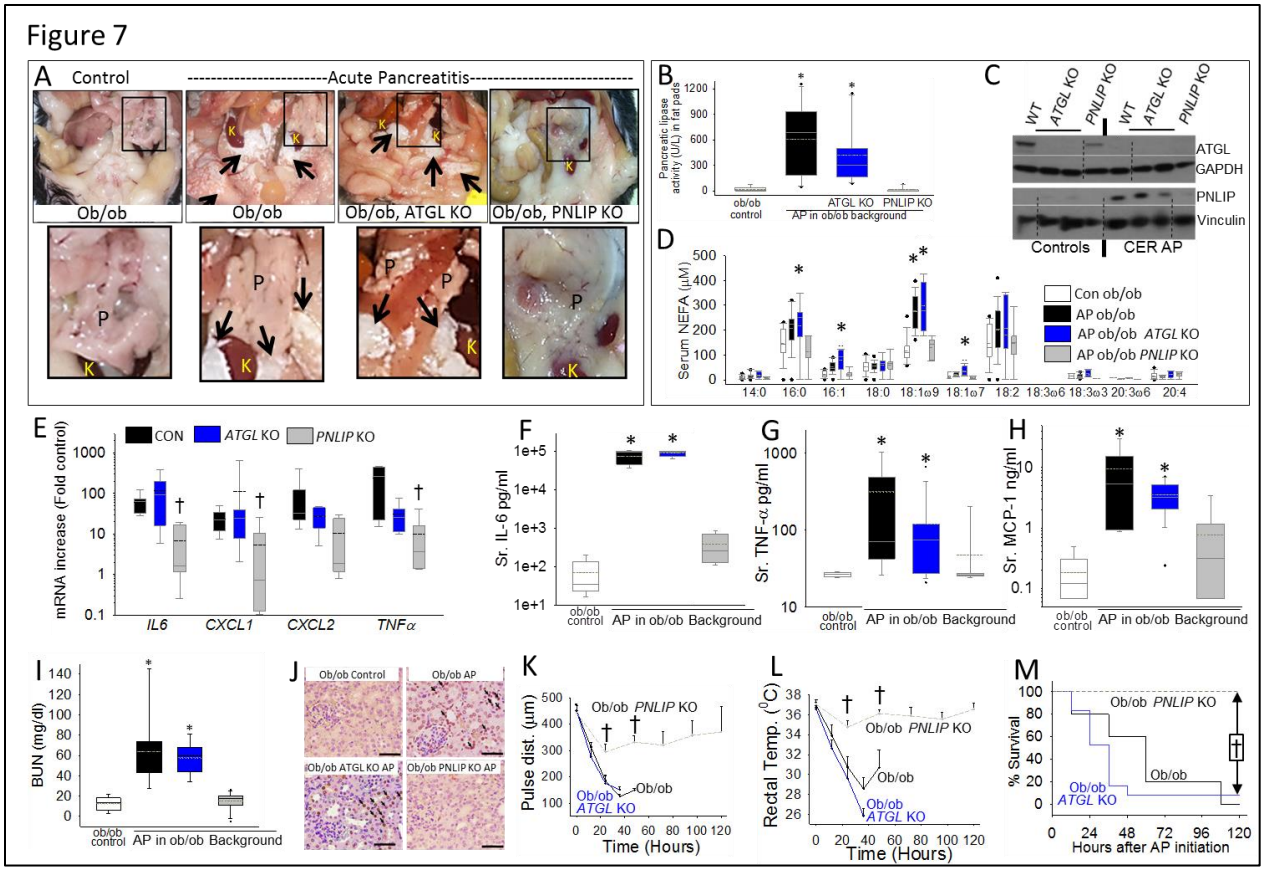

Figure 7: Inflammation and severity in ob/ob *PNLIP* KO (grey), ob/ob littermates (black) and ob/ob *ATGL* KO (blue) mice with caerulein acute pancreatitis (CER AP) A: Peritoneal cavity of controls and during pancreatitis. Black rectangle shows the pancreas, and adjacent kidney (K), perinephric fat. Note pancreas (magnified view of inset in lower panel) is edematous, lobulated in pancreatitis. Arrows highlight fat necrosis around the kidneys which is lacking in *PNLIP* KO mice. **B:** Pancreatic lipase activity in the gonadal fat pads **C**: Western blotting of visceral adipose for ATGL with GAPDH as a loading control (same gel non-contiguous) and a contempraneously run gel for PNLIP with a vinculin loading control (same gel noncontiguous). Dotted lines depict spilicing (**D**) Serum NEFA in pancreatitis and controls (white bar). (**E**) mRNA levels of cytokines in the visceral adipose tissue from mice with pancreatitis shown a fold of the levels in control mice without pancreatitis. Serum IL-6 (**F**), TNF-α (**G**), MCP-1 (**H**), BUN (**I**) in the various groups. * indicates a P<0.05 by ANOVA vs. controls without pancreatitis. Box plots depict mean (dashed line), median (solid line), 25th and 75th percentiles (2 boxes), 10th and 90th percentiles (whiskers), and outliers (dots). **J**: Kidney TUNEL staining (brown nuclei, arros highlight some) ofthe various groups. Note the increase in the ob/ob and ob/ob *ATGL* KO mice with pancreatitis. The scale bars at the bottom measure 100μm. Trends of the carotid pulse distension (**K**) to measure shock, rectal temperature (**L**) to measure organ failure (shown as mean ± SEM), and survival (**M**) in the various groups. The dashed lines are *PNLIP* KO mice with pancreatitis. * indicates a *P*<0.05 by ANOVA vs. other groups. †indicates a significant reduction in the ob/ob *PNLIP* KO group with acute pancreatitis vs. the ob/ob group on ANOVA. Each group had 8-10 mice.

Figure 8

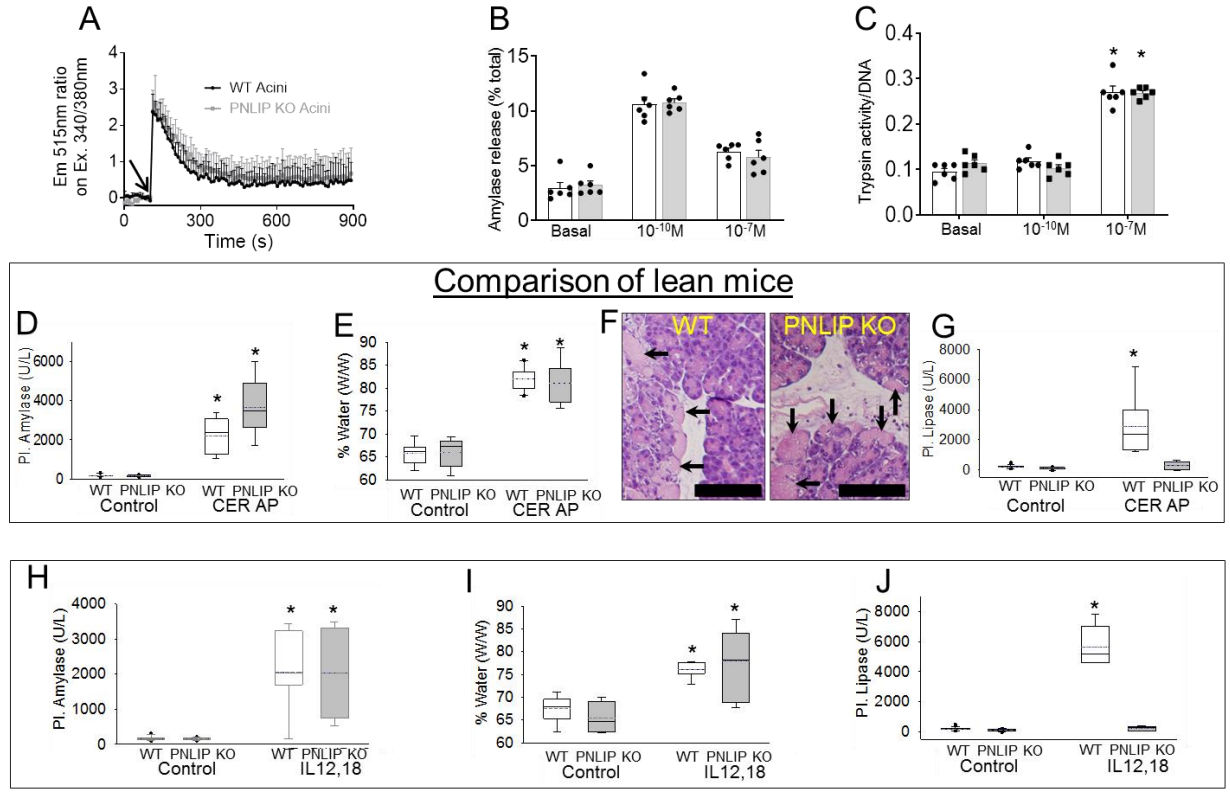

Figure 8: Comparison of acinar cell signaling and early events during pancreatitis in *PNLIP* KO (grey) vs. wild type mice (WT, black). A: Cytosolic calcium increase in response to 100nM caerulein (arrow) as measured in Fura-2AM loaded acini, (mean±SEM of 4 different experiments) **B:** Comparison of physiologic amylase release into the medium **(B)** and pathologic trypsinogen activation to trypsin (**C)** in response to physiologic (10^{-10} M) and supraphysiologic (pathologic; 10^{-7} M) doses of caerulein. Each pont represents a separate experiment. Circulating amylase (**D)**, pancreatic edema measured as % weight of water to pancreatitis wet weight **(E).** Pancreatic histology showing necrosis (arrows)**.** The scale bars at the bottom measure 50μm **(F).** Circulating pancreatic lipase **(G)** levels measured at the end of 10 hours of caerulein acute pancreatitis vs. controls. Note similar parameters in the two groups, except lipase. Circulating amylase (**H)**, pancreatic edema in control mice and at the time of necropsy after IL12, 18 acute pancreatitis **(I)** and circulating pancreatic lipase **(J)** levels measured after 24 hours of the first IL12,18 injection. Note similar parameters in the two groups, except lipase. Box plots depict mean (dashed line), median (solid line), 25th and 75th percentiles (2 boxes), 10th and 90th percentiles (whiskers), and outliers (dots). * indicates a P<0.05 by vs. controls or basal levels. Each group had 8-10 mice.

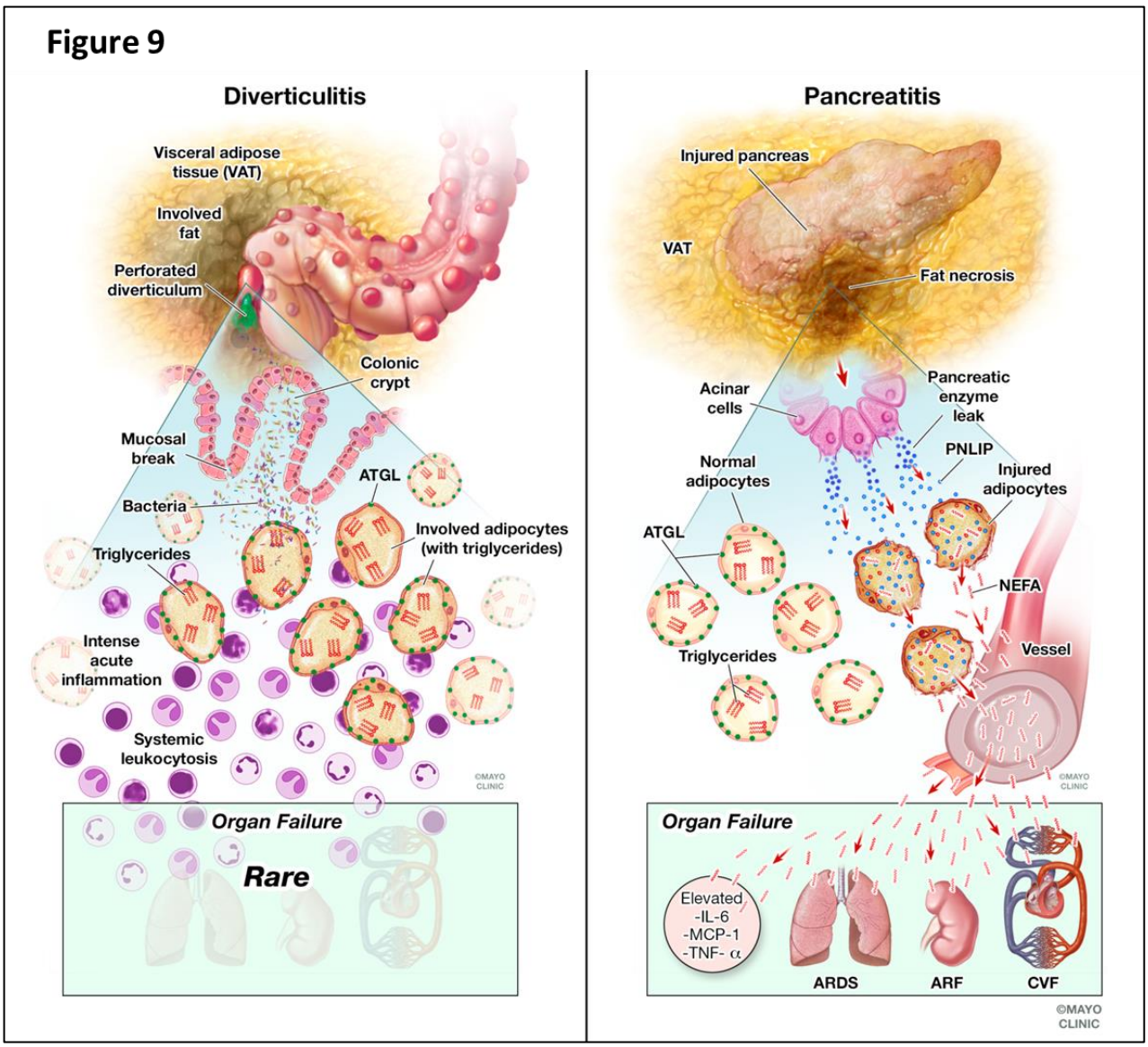

Figure 9: Diagrammatic representation of the difference in pathophysiology of acute diverticulitis and acute pancreatitis. Shown here are the pathophysiology explaining the histological, biochemical and clinical findings noted in diverticulitis (left) and pancreatitis (right). In the upper part of the left iamge is shown a perforated diverticulum in the colon with spillage of contents into the visceral adipose tissue. In the lower panel is the zoomed in view showing the consequent intense local inflammation in the peri-colonic visceral adipose tissue. However the triglyceride (red E) within adipocytes is not degraded and the ATGL (green dots) remains intact. This is associated with a low prevalence of organ failure during diverticulitis. On the right, is shown the involvement of visceral adipose tissue in pancreatitis, with the zoomed in view at the bottom showing the leakage of pancreatic enzymes (dark blue) including PNLIP (light blue) into the visceral adipose tissue. The resulting adipocyte injury results in entry of PNLIP into the injured adipocytes resulting in hydrolysis of adipocyte triglyceride into NEFA (red wavy lines), and degradation of ATGL seen as loss of green dots. The entry of NEFA into the systemic circulation causes elevated cytokines, organ failure including acute respiratory distress syndrome (ARDS), acute renal failure (ARF), and cardiovascular failure (CVF).

Table 1:

Parameter	Control patients (15)	Severe AP patients (15)	*P* value
Race (B:W)	1:14	0:15	1.0
Age	50.0±12.1	52.8±12.0	0.52
Sex (M:F)	5:10	10:5	0.14
BMI	30.3±7.9	34.2±5.4	0.13
Organ failure	0/15	15/15	0.0001

Table 1: Table comparing the demographics and presence of organ failure in human normal controls and patients with severe acute pancreatitis (AP) whose blood levels of oleic acid were measured.

SUPPLEMENTARY MATERIALS:

Methods:

- Non-esterified fatty acid (NEFA) and visceral fat triglycerides analysis
- Cytokine and Chemokine Assays
- Biochemistry assays
- Western blot analysis
- Lipase, amylase and trypsin activity in tissue homogenates
- TLC protocol
- Recombinant proteins
- 3T3-L1 cell culture and use
- Adipocyte and acinar cell isolation and use

Figures:

Figure S1: Demographics and clinical parameters of the acute pancreatitis and acute diverticulitis patients.

Figure S2: Temporal course of the increase of pancreatic lipases in visceral adipose tissue, showing its correlation with fat necrosis, acute pancreatitis severity and loss of adipocyte proteins.

Figure S3: Images of the peritoneal cavities of lean (C57bl/6) mice with (B-D) and without caerulein acute pancreatitis (A).

Figure S4: Mechanisms by which adipocyte cell membranes may be compromised to allow entry of PNLIP into the cell.

Figure S5: Effect of the ATGL inhibitor (Atglistatin 50μM) and *ATGL* KO adipocytes on isoproterenol (Iso) induced glycerol release.

Figure S6: Histologic appearance of serial formalin fixed paraffin embedded section from caerulein pancreatitis and surrounding fat after Hematoxylin and eosin (H&E; Left) and von-Kossa staining (right) for calcium. The groups are mentioned on the left side.

Figure S7: Parent images of the sections shown in Figure 6F.

Figure S8: A: Thin layer chromatography of fat pads of mice with pancreatitis (AP). To the left are the standards of the 3 lipid classes. B: Sirius red images of the pancreas showing fibrosis.

Figure S9: Masson's trichrome stained images of the various groups.

Figure S10: TUNEL stained images of the lungs from different groups of mice.

Figure S11: Comparison of ob/ob *PNLIP* KO (grey) and ob/ob mice (black) for IL12, 18 AP mediated parameters of pancreatic injury, fat necrosis, NEFA generation, inflammatory response, organ failure, and survival.

Figure S12: Effect of *PNLIP* KO on caerulein AP in lean mice and early (24-hour) IL12-, 18-induced pancreatitis.